

Melanophilin mediates the association of myosin-5a with melanosome via three distinct interactions

Reviewed Preprint

Revised by authors after peer review.

[About eLife's process](#)

Reviewed preprint version 2

May 16, 2024 (this version)

Reviewed preprint version 1

January 19, 2024

Posted to preprint server

November 4, 2023


Sent for peer review

November 1, 2023

Jiabin Pan, Rui Zhou, Lin-Lin Yao, Jie Zhang, Ning Zhang, Qin-Juan Cao, Shaopeng Sun, Xiang-dong Li 

Group of Cell Motility and Muscle Contraction, State Key Laboratory of Integrated Management of Pest Insects and Rodents, Institute of Zoology, Chinese Academy of Sciences, Beijing 100101, China • University of Chinese Academy of Sciences, Beijing 100049, China

 https://en.wikipedia.org/wiki/Open_access

 Copyright information

Abstract

Transport and localization of melanosome at the periphery region of melanocyte are depended on myosin-5a (Myo5a), which associates with melanosome by interacting with its adaptor protein melanophilin (Mlph). Mlph contains four functional regions, including Rab27a-binding domain, Myo5a GTD-binding motif (GTBM), Myo5a exon F-binding domain (EFBD), and actin-binding domain (ABD). The association of Myo5a with Mlph is known to be mediated by two specific interactions: the interaction between the exon-F-encoded region of Myo5a and Mlph-EFBD and that between Myo5a-GTD and Mlph-GTBM. Here, we identify a third interaction between Myo5a and Mlph, i.e., the interaction between the exon-G-encoded region of Myo5a and Mlph-ABD. The exon-G/ABD interaction is independent from the exon-F/EFBD interaction and is required for the association of Myo5a with melanosome. Moreover, we demonstrate that Mlph-ABD interacts with either the exon-G or actin filament, but cannot interact with both of them simultaneously. Based on above findings, we propose a new model for the Mlph-mediated Myo5a transportation of melanosomes.

eLife assessment

This study represents a **useful** description of a third interaction site between melanophilin and myosin-5a which has a role in regulating the distribution of pigment granules in melanocytes. While much of the data forms a **solid** case for this interaction, the inclusion of controls for the cellular studies and measurement of interaction affinities would have been helpful.

<https://doi.org/10.7554/eLife.93662.2.sa2>

Introduction

Melanosome is a specialized organelle within which melanin pigments are synthesized and stored. The peripheral accumulation of melanosomes in melanocytes is essential for the intercellular transfer of the organelles from the dendrite tips of melanocytes to the adjacent keratinocytes

(Hume & Seabra, 2011 [↗](#)). Microtubule and the associated motor proteins are responsible for the long-range and bidirectional transport of melanosomes between the nucleus to cell periphery, and actin filament and the associated motor protein myosin-5a (Myo5a) are essential for the short-distance transport and the capture of melanosomes at cell periphery (Wu et al., 1998 [↗](#); Wu & Hammer, 2014 [↗](#)). The overall effect of the two transport systems is the peripheral accumulation of melanosomes in melanocytes. Lack of the latter causes the perinuclear accumulation of melanosomes in melanocytes, a phenotype called “dilute” (Provance et al., 1996 [↗](#); Wei et al., 1997 [↗](#)).

Myo5a is a processive motor that has been implicated in the transportation and the tethering of organelles along actin filaments (Lindsay & McCaffrey, 2014 [↗](#); Mehta et al., 1999 [↗](#); Rudolf et al., 2011 [↗](#); Yoshimura et al., 2006 [↗](#); Zhang et al., 2018 [↗](#)). Myo5a has two heavy chains, each containing an N-terminal motor domain, six IQ motifs that act as the binding sites for calmodulin (CaM) or CaM-like light chains, and a tail (Ikebe, 2008 [↗](#); Zhang et al., 2018 [↗](#)). The tail of Myo5a can be further divided into three segments. The proximal tail is a long coiled-coil with length about 200 residues. The distal tail is the C-terminal globular tail domain (GTD). Between the proximal tail and the GTD is the middle tail, which is comprised of several short coiled-coils and the connecting loops. At least three essential functions are served by Myo5a tail. First, the coiled-coil regions enable Myo5a to form a dimer. Second, the GTD inhibits the motor activity of myosin head. Third, the tail is the binding site for the cargo proteins. The motor activity of Myo5a is tightly regulated (Krementsov et al., 2004 [↗](#); Li et al., 2006 [↗](#); Li et al., 2008 [↗](#); Li et al., 2004 [↗](#); Liu et al., 2006 [↗](#); Thirumurugan et al., 2006 [↗](#); Wang et al., 2004 [↗](#)). In the inhibited state, Myo5a forms a folded conformation, in which the GTDs fold back to interact and inhibit the motor function. Upon being activated by high Ca^{2+} , cargo or adaptor proteins, Myo5a transforms from the folded conformation to the extended conformation, in which the GTD dissociates from the motor domain and the inhibition is relieved.

Melanophilin (Mlph) is one of the best-studied cargo proteins of Myo5a. Together with Rab27a, Mlph mediates the attachment of Myo5a to melanosomes. Rab27a is a small GTPase that, in the GTP-bound form, is anchored into the melanosome membrane via its lipid moiety (Ishida et al., 2014 [↗](#); Wandinger-Ness & Zerial, 2014 [↗](#)) and Mlph bridges the interaction between Rab27a and Myo5a (Fukuda et al., 2002 [↗](#); Nagashima et al., 2002 [↗](#); X. S. Wu et al., 2002 [↗](#)). The tripartite complex of Rab27a, Mlph, and Myo5a connects the melanosome to the actin filament. Lacking any one of these three components in melanocytes causes dilute phenotype (perinuclear accumulation of melanosomes) (Fukuda et al., 2002 [↗](#); Hume et al., 2001 [↗](#); Strom et al., 2002 [↗](#); Wei et al., 1997 [↗](#); Wu et al., 2001 [↗](#); X. S. Wu et al., 2002 [↗](#)).

Mlph contains four functional regions, including RBD (Rab27a-binding domain), GTBM (Myo5a GTD-binding motif), EFBD (Myo5a exon F-binding domain), and ABD (actin-binding domain) (Fukuda et al., 2002 [↗](#); Geething & Spudich, 2007 [↗](#); Li et al., 2005 [↗](#); Yao et al., 2015 [↗](#)). The association of Myo5a with Mlph involves two molecular interactions. One is the interaction between the exon-F-encoded region (exon-F for simplification) of Myo5a and the EFBD of Mlph (Fukuda & Itoh, 2004 [↗](#); X. Wu et al., 2002 [↗](#); X. S. Wu et al., 2002 [↗](#)). Exon-F is an alternatively spliced exon presents in the middle tail of the melanocyte-spliced isoform of Myo5a (Huang et al., 1998 [↗](#)). The exon-F/EFBD interaction is absolutely essential for the localization of Myo5a to the melanosome (X. Wu et al., 2002 [↗](#)). The other interaction is between the GTD of Myo5a and the GTBM of Mlph (Geething & Spudich, 2007 [↗](#); Pylypenko et al., 2013 [↗](#); Wei et al., 2013 [↗](#)). We previously found that GTBM activates Myo5a motor function by relieving the GTD inhibition on the motor domain and inducing a folded-to-extended conformational transition of Myo5a (Li et al., 2005 [↗](#); Yao et al., 2015 [↗](#)). Recently, we demonstrated that the activation of Myo5a by Mlph-GTBM is regulated by another Myo5a-binding protein RILPL2 (Rab-interacting lysosomal protein-like 2) and the small GTPase Rab36, a binding partner of RILPL2 (Cao et al., 2019 [↗](#)).

Mlph-ABD is essential to proper melanosome transport (Fukuda & Kuroda, 2002 [↗](#); T. S. Kuroda et al., 2003 [↗](#); Taruho S. Kuroda et al., 2003 [↗](#)). Besides being able to bind to actin filament, Mlph-ABD could interact with end-binding protein 1, which might facilitate the transfer of melanosomes from microtubules to actin (Wu et al., 2005 [↗](#)). *In vitro* motility assays at single-molecular level show that Mlph prolongs and slows the processive movements of Myo5a, presumably via the interaction between ABD and actin filament (Sckolnick et al., 2013 [↗](#)). A cluster of conserved positively charged residues in ABD is essential for actin binding and Melanophilin localization in melanocytes (T. S. Kuroda et al., 2003 [↗](#)). An *in vitro* study suggests that Mlph-ABD is a target of protein kinase A and that the phosphorylated Mlph preferred binding to actin even in the presence of microtubules, whereas dephosphorylated Mlph bind to microtubules (Oberhofer et al., 2017 [↗](#)).

Biochemical analysis of Mlph show that the ABD is not essential for the interaction with Myo5a nor the activation of Myo5a motor function, suggesting that a truncated Mlph protein containing the RBD and the two Myo5a-binding domains (the GTBM and the EFBD) but lacking the ABD is able to form a tripartite complex with Rab27a and Myo5a and thus sufficient for the recruitment of Myo5a to melanosome membrane (T. S. Kuroda et al., 2003 [↗](#); X. Wu et al., 2002 [↗](#)). However, using melan-In cells (Mlph-null melanocytes), Hume et al. have found that the ABD-deleted Mlph cannot to promote the recruitment of Myo5a onto melanosomes, indicating that the ABD is necessary *in situ* for the association of Myo5a with Mlph (Hume, 2006 [↗](#)). This discrepancy between *in vitro* and cell culture results promoted us to investigate the interaction between Mlph-ABD and Myo5a.

In this study, we have identified a third interaction between Myo5a and Mlph, i.e., the interaction between the exon-G-encoded region (exon-G for simplification) of Myo5a and Mlph-ABD. We find that the exon-G/ABD interaction is independent from the exon-F/EFBD interaction, and that, similar to exon-F/EFBD, exon-G/ABD is essential for the dilute-like phenotype induced by Myo5a-tail overexpression. Moreover, we demonstrate that Mlph-ABD interacts with either the exon-G of Myo5a or actin filament, but cannot interact with both of them simultaneously. Based on above findings, we propose a new model for the Mlph-mediated Myo5a transportation of melanosomes.

Results

The actin-binding domain of melanophilin (Mlph-ABD) contains a novel Myo5a-binding site

Myo5a binds to its cargo proteins, including Mlph, majorly via the middle tail domain (MTD, residues 1106-1467) and the GTD (residues 1468-1877) (Figure 1A [↗](#), top). The C-terminal portion of the MTD is encoded by a serial exons, called exon-A to -G, among which exon-B, -D, and -F are alternatively spliced exons (Seperack et al., 1995 [↗](#)). The melanocyte isoform of Myo5a contains exon-D and -F (Figure 1A [↗](#), middle), whereas the brain isoform contains exon-B. The MTD is predicted to form four short coiled-coils, among which the last one is formed by the C-terminus of exon-F and the entire exon-G (Figure 1 [↗](#) A, bottom).

To detect interaction between the ABD of Mlph with Myo5a, we performed GST pulldown assay using GST-Mlph-ABD (the GST-tagged ABD of Mlph, residues 401-590) and Flag-Myo5a-MTD (the Flag-tagged middle tail domain of Myo5a, residues 1106-1467) (Figure 1A [↗](#) and 1B [↗](#)). GST-Mlph-ABD was expressed in *E. coli* and purified by GSH-Sepharose chromatography, and Flag-Myo5a-MTD was expressed in Sf9 cells and purified by anti-Flag affinity chromatography. GST pulldown assay shows that GST-Mlph-ABD specifically interacted with Flag-Myo5a-MTD (Figure 1C [↗](#), lane 2). Deleting the residues 401-437 of Mlph-ABD had little effect on the interaction with Myo5a-MTD (Figure 1C [↗](#), lane 3 and 4), indicating the N-terminal 37 residues of Mlph-ABD are not essential for the interaction. Further deletion of 437-446 slightly decreased the interaction and deletion of 446-455 eliminated the interaction (Figure 1C [↗](#), lane 5 and 6), indicating that residues 446-455 are

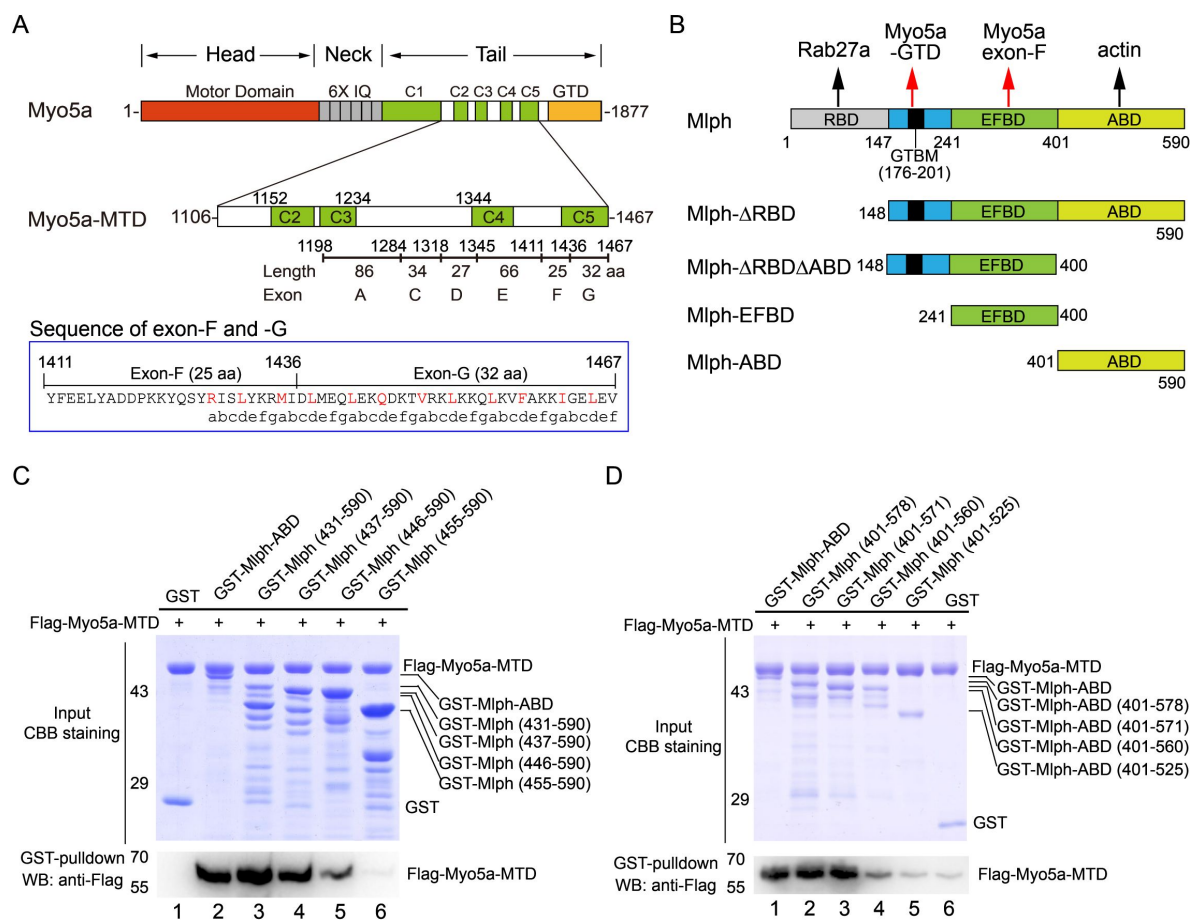


Figure 1.

The actin-binding domain of melanophilin (Mlph-ABD) interacts with the middle tail domain (MTD) of Myo5a.

(A) Diagram of the melanocyte-spliced isoform of Myo5a. Myo5a-MTD, Myo5a coiled-coils (residues 1106-1469). IQ, the CaM binding site; GTD, the C-terminal globular tail domain. In blue box is the sequence of exon-F and -G, annotated with the predicted coiled-coil heptad repeats. (B) Diagram of melanophilin (Mlph). RBD, Rab27a-binding domain; GTBM, globular tail domain-binding motif; EFBD, exon-F binding domain; ABD, actin-binding domain. (C, D) GST pull-down of GST-Mlph-ABD with the N-terminus truncated (C) or the C-terminus truncated (D) with Flag-Myo5a-MTD. GST-Mlph-ABD constructs were bound to GSH-Sepharose and then incubated with Flag-Myo5a-MTD. The GSH-Sepharose-bound proteins were eluted by GSH and analyzed by Western blot using anti-Flag antibody. The inputs were analyzed with SDS-PAGE and visualized by Coomassie brilliant blue (CBB) staining. GST was used as negative control. Note: The Sf9 cell-expressed Myo5a-MTD was used in the GST pull-down assays shown in this figure.

Figure 1-Source data 1 Original and uncropped gels and blots for **Figure 1C**.

Figure 1-Source data 2 Original and uncropped gels and blots for **Figure 1D**.

essential for the interaction with Myo5a-MTD. Similarly, we performed C-terminal truncation analysis of Mlph-ABD on the interaction with Myo5a-MTD and identified residues 560-571 essential for the interaction (Figure ID). Taking together, we identified the middle portion of Mlph-ABD (residues 446-571) as the core of the novel binding site for Myo5a-MTD.

We then produced a number of truncated Myo5a-MTD constructs and performed GST pulldown assays to narrow down the region in Myo5a-MTD binding to Mlph-ABD (Figure 2A). To simplify the experiments, we first compared the bacterial-expressed Myo5a-MTD with the Sf9 cell-expressed Myo5a-MTD in the interaction with Mlph-ABD. GST pulldown assay shows that both versions of Myo5a-MTD specifically interacted with Mlph-ABD (Figure 2-figure supplement A). All the following pulldown experiments were performed using the bacterial-expressed Myo5a-MTD, unless otherwise indicated. C-terminal truncation of Flag-Myo5a-MTD shows that the C-terminal half of exon-G (residues 1453-1467) is essential for binding to Mlph-ABD (Figure 2-figure supplement B). Mlph-ABD interacted strongly with Flag-Trx-Myo5a (1411-1467) (a short peptide containing exon-F and exon-G), but weakly with Flag-Trx-Myo5a (1436-1467) (a short peptide containing exon-G) (Figure 2-figure supplement C, lane 3 and 4), suggesting that exon-F might be required for strong interaction of exon-G with Mlph-ABD. However, deletion of exon-F from Myo5a-MTD did not affect the interaction with Mlph-ABD (Figure 2B, lane 2), indicating that exon-F is not essential for the interaction. Deletion of the C-terminal portion (residues 1454-1467) of exon-G abolished the binding of Myo5a-MTD with Mlph-ABD (Figure 2B, lane 3), but did not affect the interaction of Myo5a-MTD with Mlph-EFBD (Figure 2C). Figure 2A summarizes the truncation analysis of the interaction between Myo5a-MTD and Mlph-ABD. Based on above results, we conclude that the exon-G of Myo5a binds to Mlph-ABD.

Characterization of the exon-G/ABD interaction

To characterize the exon-G/ABD interaction, we monitored the interaction between Myo5a-MTD and Mlph-ABD using microscale thermophoresis (MST), and obtained the dissociation constant (K_d) of 562 ± 169 nM of Myo5a-MTD for binding to Mlph-ABD (Figure 3A). Consistent with the pulldown assay (Figure 2B), deletion of the C-terminal half of exon-G (Myo5a-MTD Δ G) greatly decreased the MST signaling (Figure 3A). We then investigated the effect of ionic strength on the exon-G/ABD interaction. GST pulldown assays of GST-Mlph-ABD and Flag-Myo5a-MTD were conducted in the presence different concentrations of NaCl. Compared with 100 mM NaCl, 300 mM and 500 mM NaCl greatly decreased the amount of Flag-Myo5a-MTD pulled down with GST-Mlph-ABD (Figure 3B), suggesting that ionic interactions are critical for the exon-G/ABD interaction.

Sequence alignment among the Mlph of mammals and birds reveals several highly conserved charged residues in the two regions of Mlph-ABD essential for the interaction with Myo5a-MTD, including four acidic residues (D447, E449, E452, and E454) in the residues 446-455 and two basic residues (R562 and R568) in the residues 560-571 (Figure 3C). To determine the roles of those conserved charged residues of Mlph on the exon-G/ABD interaction, we mutated them individually into alanine. GST pulldown assays show that both E449A and E452A mutations abolished the interaction with Myo5a-MTD, whereas other mutations (D447A, E454A, R562A, R568A) had little effect on the interaction (Figure 3E), indicating that both E449 and E452 of Mlph are essential for the exon-G/ABD interaction.

We expected the conserved acidic residues E449 and E452 of Mlph to interact with the conserved basic residues in the exon-G of Myo5a. Sequence alignment of the three Myo5 isoforms of mammals and birds reveals two highly conserved basic residues (K1456 and K1460) in the C-terminal portion of exon-G of Myo5a (Figure 3D). GST pulldown assay shows that both K1456A and K1460A mutations substantially decreased the amount of Flag-Myo5a-MTD pulled down with GST-Mlph-ABD (Figure 3F), suggesting that both K1456 and K1460 of Myo5a play a key role in the interaction with Mlph-ABD.

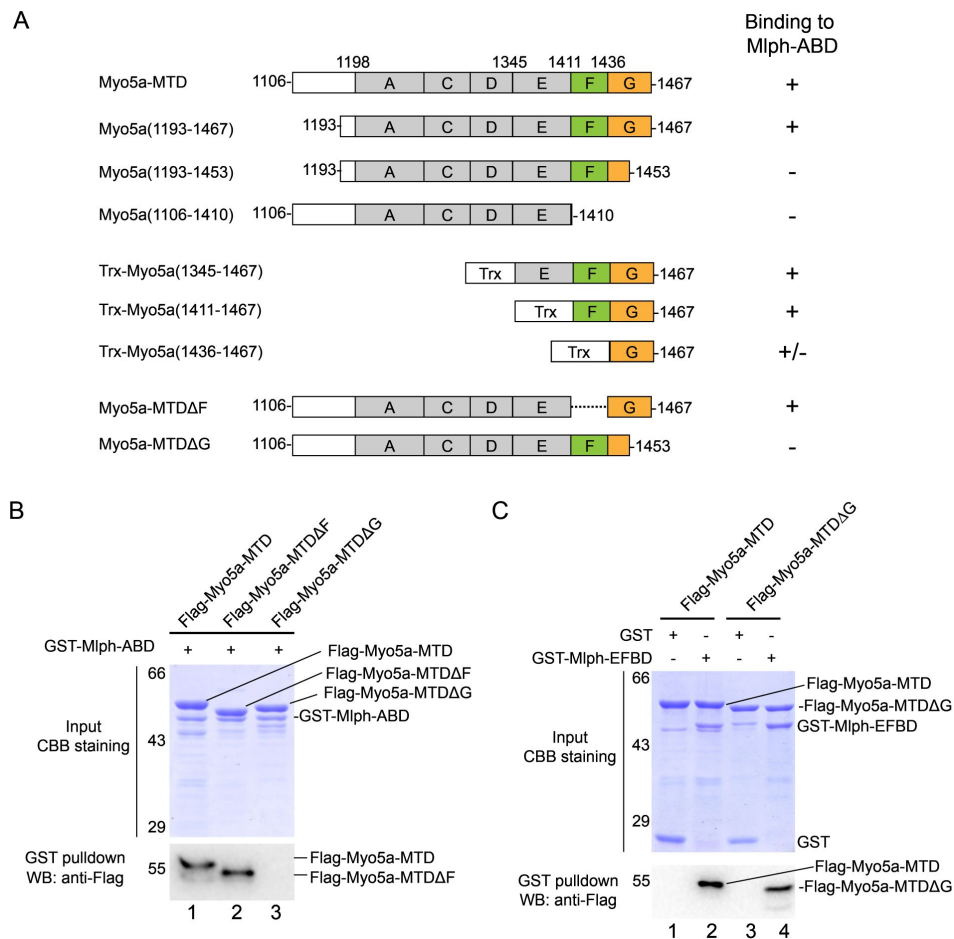


Figure 2.

The exon-G of Myo5a interacts with Mlph-ABD.

(A) Summary of the interactions between the truncated Myo5a constructs and Mlph-ABD based on the GST pull-down assay shown in Figure S1. +, strong interaction; +/-, weak interaction; -, no interaction. (B) Deletion of the C-terminal portion of exon-G abolishes the interaction between Myo5a-MTD and Mlph-ABD. (C) Deletion of the C-terminal portion of exon-G does not affect the interaction between Myo5a-MTD and Mlph-EFBD. GST pull-down assays were performed using GST-Mlph-ABD and Flag-Myo5a-MTD variants. The GSH-Sepharose-bound proteins were eluted by GSH and analyzed by Western blot using anti-FLAG antibody; the inputs were analyzed with SDS-PAGE and visualized by Coomassie brilliant blue (CBB) staining.

Figure 2-Source data 1 Original and uncropped gels and blots for **Figure 2B**.

Figure 2-Source data 2 Original and uncropped gels and blots for **Figure 2C**.

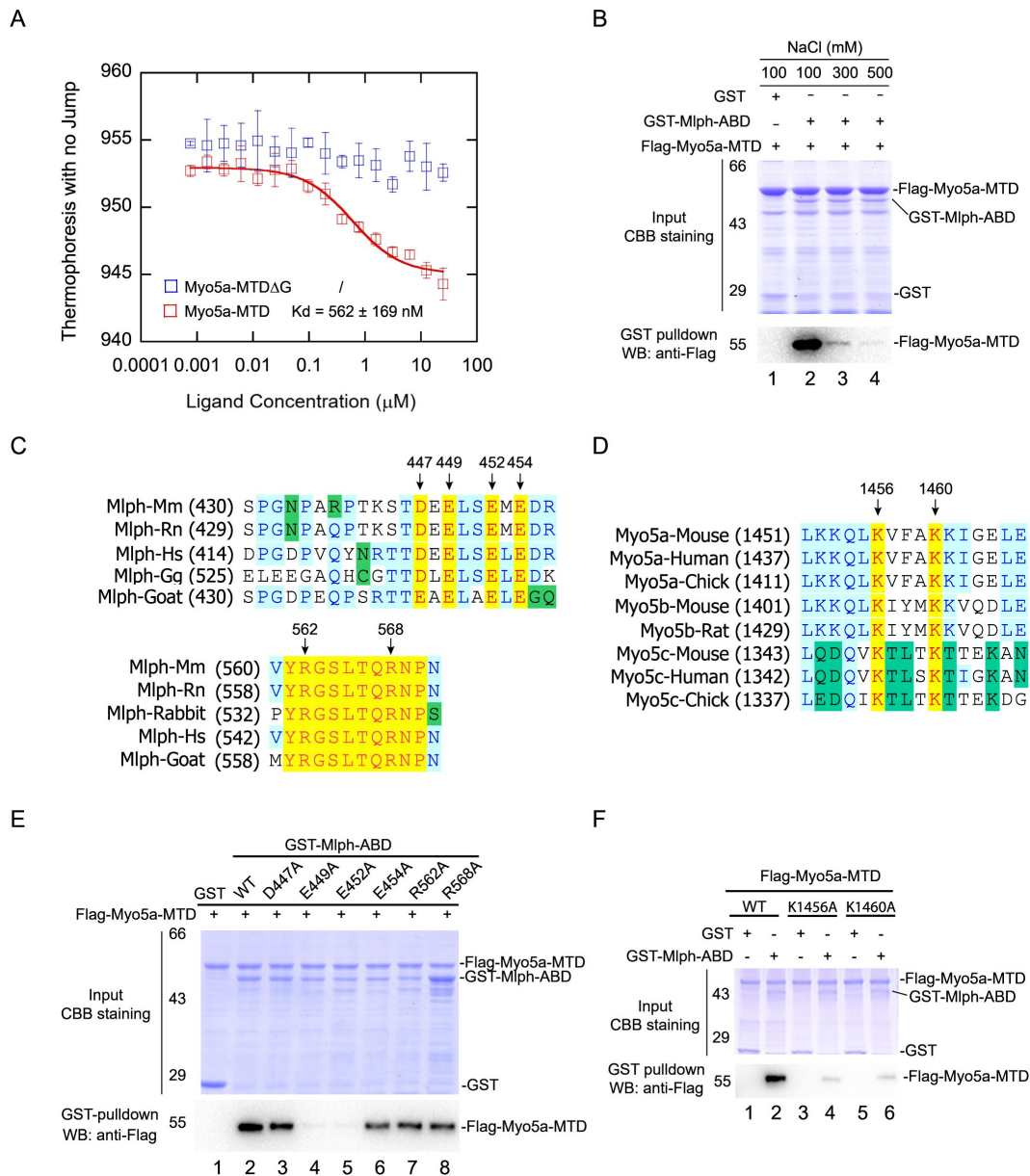


Figure 3.

Identification of the key residues for the exon-G/ABD interaction.

(A) Dissociation constant (K_d) of Myo5a-MTD or Myo5a-MTD ΔG binding to Mlph-ABD measured by MST. The solid curve was fit to the standard K_d -fit function. Bars represent Standard Error. (B) Ionic strength dependence of the interaction between Myo5a-MTD and Mlph-ABD. GST pull-down was performed using GST-Mlph-ABD and Flag-Myo5a-MTD in the presence of different concentrations of NaCl. (C) Sequence alignments of the regions in Mlph-ABD essential for binding to Myo5a-MTD. Conserved charged residues are indicated. (D) Sequence alignments of the C-terminal portion of exon-G, an essential region for binding to Mlph-ABD. Two conserved basic residues (K1456 and K1460) are indicated. (E) Effects of alanine mutation of the conserved charged residues in Mlph-ABD on the interaction with Myo5a-MTD. E449A and E452A mutations in Mlph abolished the interaction between Mlph-ABD and Myo5a-MTD. (F) Effects of K1456A and K1460A mutations of Myo5a-MTD on the interaction with Mlph-ABD.

Figure 3-Source data 1 Original MST data for **Figure 3A**.

Figure 3-Source data 2 Original and uncropped gels and blots for **Figure 3B**.

Figure 3-Source data 3 Original and uncropped gels and blots for **Figure 3E**.

Figure 3-Source data 4 Original and uncropped gels and blots for **Figure 3F**.

The exon-F/EFBD interaction and the exon-G/ABD interaction are independent from each other

Because exon-F and exon-G are in immediate vicinity, it is possible that the exon-F/EFBD interaction and the exon-G/ABD interaction interfere with each other. To test this possibility, we performed GST pulldown assays of GST-Mlph-ABD and Flag-Mlph-EFBD in the presence or absence of Flag-Myo5a-MTD. If Myo5a-MTD is able to interact with both Mlph-ABD and Mlph-EFBD simultaneously, a tripartite complex will be formed by Myo5a-MTD, Mlph-ABD, and Mlph-EFBD (**Figure 4A** [↗](#), upper panel), and Flag-Mlph-EFBD will be pulled down with GST-Mlph-ABD in the presence of Flag-Myo5a-MTD. As shown in **Figure 4A** [↗](#), Flag-Mlph-EFBD was pulled down with GST-Mlph-ABD in the presence of Flag-Myo5a-MTD, but not in the absence of Flag-Myo5a-MTD. This result is consistent with a scenario that Myo5a-MTD binds to both Mlph-EFBD and Mlph-ABD simultaneously. We therefore conclude that the exon-F/EFBD interaction and the exon-G/ABD interaction do not interfere with each other.

As the exon-F/EFBD interaction and the exon-G/ABD interaction are independent to each other, we expected that those two interactions act synergically for the binding of Myo5a-MTD to Mlph. As expected, GST pulldown assays show that GST-Mlph- Δ RBD, which contains both EFBD and ABD, strongly bound to Flag-Myo5a-MTD, and deletion of either exon-F or exon-G from Myo5a-MTD substantially weakened the interaction with GST-Mlph- Δ RBD (**Figure 4B** [↗](#)). Conversely, Flag pulldown shows that substantial amount of GST-Mlph- Δ RBD could be pulled down with Flag-Myo5a-MTD, and deleting ABD from GST-Mlph- Δ RBD strongly decreased the amount of protein pulled down with Flag-Myo5a-MTD (**Figure 4C** [↗](#)). Above results indicate that the exon-F/EFBD interaction and the exon-G/ABD interaction act synergically, resulting in a strong interaction between Myo5a-MTD and Mlph.

Mlph-ABD cannot interact with F-actin and exon-G simultaneously

In addition to interacting with the exon-G of Myo5a, Mlph-ABD is able to bind to actin. To investigate whether Mlph-ABD interacts with actin and exon-G simultaneously, we performed actin co-sedimentation of Mlph-ABD and Myo5a-MTD. As expected, substantial amount of Mlph-ABD, but essentially no Myo5a-MTD, was co-sedimentated with F-actin (**Figure 5A** [↗](#)). Interestingly, Mlph-ABD did not increase the amount of Myo5a-MTD co-sedimentated with F-actin (**Figure 5A** [↗](#)), suggesting that Mlph-ABD cannot interact with F-actin and exon-G simultaneously.

The inability of Mlph-ABD to interact with F-actin and exon-G simultaneously suggests that F-actin and exon-G compete in binding to Mlph-ABD. It is possible that Myo5a-MTD might antagonize the interaction between Mlph-ABD and F-actin. To test this possibility, we performed F-actin co-sedimentations of Mlph-ABD in the presence of different concentrations of Myo5a-MTD. As expected, Myo5a-MTD substantially decreased the amount of Mlph-ABD co-sedimentated with F-actin (**Figure 5B** [↗](#)). We therefore concluded that Mlph-ABD cannot bind to F-actin and exon-G simultaneously and those two interactions are mutually exclusive.

The exon-G/ABD interaction is essential for Myo5a-tail to induce dilute-like phenotype in melanocytes

Myo5a associates with melanosome via its interaction with Mlph, which attaches to melanosome via the interaction between its RBD and the melanosome-bound Rab27a. Overexpression of the EGFP fusion protein of Mlph- Δ RBD in the melanocyte cell line, melan-a, caused dilute-like phenotype, i.e., the perinuclear distribution of melanosomes in melanocyte (**Figure 6A** [↗](#), **Figure 6-figure supplement** [↗](#)). Generation of dilute-like phenotype by Mlph- Δ RBD was attributed to the ability of Mlph- Δ RBD to compete with the melanosome-bound Mlph in interacting with Myo5a molecules, thereby dissociating Myo5a from melanosome. To investigate whether the exon-G/ABD interaction is essential for the dominant negative effect of Mlph- Δ RBD in melanocyte, we

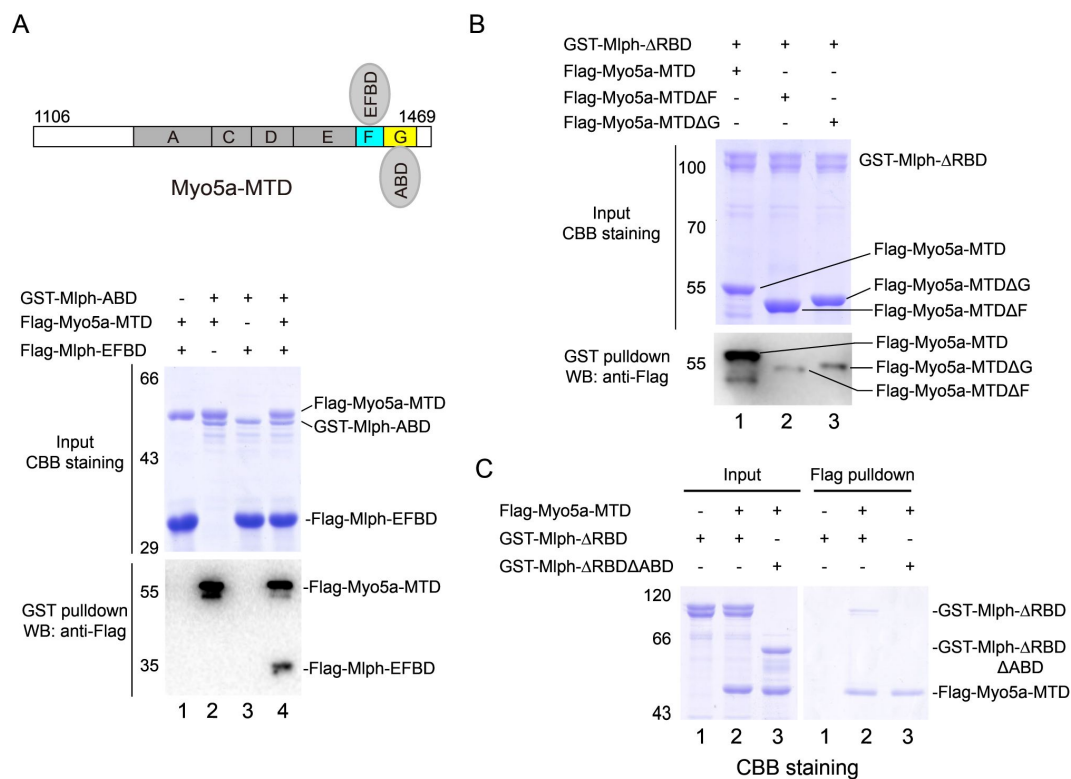


Figure 4.

The exon-F/EFBD and the exon-G/ABD interactions act synergistically.

(A) Myo5a-MTD bridges between Mlph-ABD and Mlph-EFBD. Upper, diagram shows Myo5a-MTD binds to both the EFBD and the ABD of Mlph. Lower, GST pull-down assays of GST-Mlph-ABD and Flag-Mlph-EFBD with or without Flag-Myo5a-MTD. (B) Both exon-F and exon-G of Myo5a-MTD are required for the strong interaction with Mlph-ΔRBD. GST pull-down of GST-Mlph-ΔRBD with Flag-Myo5a-MTD variants. (C) ABD is essential for the strong interaction between Mlph-ΔRBD and Myo5a-MTD. The input samples were analyzed by SDS-PAGE and visualized by CBB staining. The pulled down samples were analyzed by Western blot using anti-Flag antibody (A and B) or by SDS-PAGE with CBB staining (C).

Figure 4-Source data 1 Original and uncropped gels and blots for **Figure 4A**.

Figure 4-Source data 2 Original and uncropped gels and blots for **Figure 4B**.

Figure 4-Source data 3 Original and uncropped gels for **Figure 4C**.

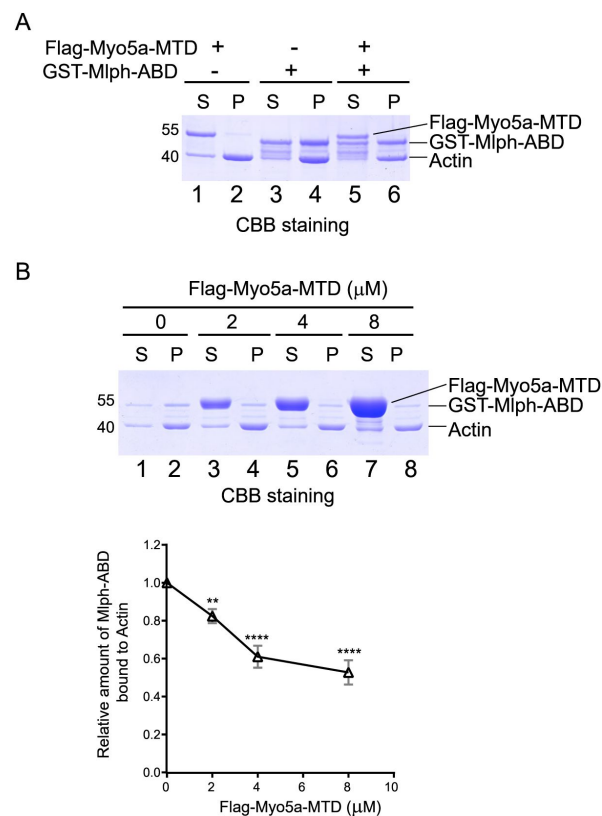


Figure 5.

Myo5a-MTD antagonizes the interaction between Mlph-ABD and actin.

(A) GST-Mlph-ABD and/or Flag-Myo5a-MTD were incubated with actin and then subjected to ultracentrifugation. The supernatants (S) and the pellets (P) were analyzed by SDS-PAGE (10%) with CBB staining. (B) GST-Mlph-ABD was incubated with actin in the presence of different concentrations of Flag-Myo5a-MTD and then subjected to ultracentrifugation. Upper panel, the supernatants (S) and the pellets (P) were analyzed by SDS-PAGE (10%) with CBB staining. Lower panel, the amounts of GST-Mlph-ABD co-sedimentated with actin in the presence of different concentration of Flag-Myo5a-MTD were quantified based on the density in the SDS-PAGE. Data are the mean \pm SD of three independent experiments with one-way ANOVA with post-hoc Bonferroni test. ** $p < 0.01$, **** $p < 0.0001$. Note: a Sf9 cell-expressed Myo5a-MTD was used in the actin cosedimentation assays shown in this figure.

Figure 5-Source data 1 Original and uncropped gels for **Figure 5A**.

Figure 5-Source data 2 Original and uncropped gels and statistical data for **Figure 5 B**.

introduced two single pointed mutations, E449A and E452A, in Mlph- Δ RBD, both of which are essential for Mlph-ABD to interact with the exon-G (**Figure 3E**). We found that both two mutations substantially decreased the number of the transfected cells with dilute-like phenotype. While dilute-like phenotype was presented in 48.78% of cells expressing the wild-type Mlph- Δ RBD, only in 20.97% and 19.07% of cells expressing E449A and E542A, respectively (**Figure 6B**). Western blots of the lysate of transfected cells showed no degradation of the expressed proteins of EGFP-Mlph- Δ RBD WT and two mutants (**Figure 6C**). Based on the band densities in the Western blot and the transfection efficiencies of those three constructs, we estimated the relative protein expression levels of each transfected cells for EGFP-Mlph- Δ RBD WT, E449A, and E452A were roughly equal (**Figure 6C**). Therefore, we conclude that the inability of E449A and E452A mutants to generate dilute-like phenotypes was not due to the intracellular degradation or the low expression level of the EGFP fusion proteins.

To further determine the role of the exon-G/ABD interaction on the tethering of Myo5a with Mlph in melanocyte, we expressed the EGFP fusion protein of Myo5a-tail (residues 1106-1877), which contains all three Mlph-binding regions, i.e., exon-F, exon-G, and GTD (**Figure 7A**). Overexpressing the tail region of Myo5a in melanocyte was expected to compete with endogenous Myo5a in interacting with Mlph, thus causing dilute-like phenotype (Wu et al 2002). Deletion analysis of the tail region of Myo5a have shown that both exon-F and the GTD are required and that neither of them alone is sufficient for generating the dominant negative phenotype in melanocytes (Wu et al 2002). Similar to the previous report, Myo5a-tail is well co-localized with both melanosome and Mlph, and generated dilute-like phenotype in ~50% of transfected melan-a melanocytes (**Figure 7B** and **7C**). In contrast, Myo5a-Tail Δ G generated dilute-like phenotype in only ~10% of transfected cells (**Figure 7B** and **7C**, **Figure 7-figure supplement**). Western blot of the lysate of transfected cells showed no degradation of the expressed proteins of EGFP-Myo5a-Tail WT and Δ G (**Figure 7D**). Based on the band densities in the Western blot and the transfection efficiencies, we estimated the relative protein expression levels of each transfected cells for EGFP-Myo5a-Tail WT and Δ G were roughly equal. Therefore, we conclude that the inability of EGFP-Myo5a-Tail Δ G to generate dilute-like phenotypes was not due to the intracellular degradation or the low expression level of the EGFP fusion protein.

Based on above results, we concluded that, similar to exon-F, exon-G is also required for Myo5a-Tail to disrupt endogenous Myo5a function in transportation of melanosomes.

Myo5a-MTD colocalized with Mlph but was unable to induce dilute-like phenotype

Unlike Myo5a-Tail, overexpression of Myo5a-MTD, which contains both exon-F and exon-G but lacks the GTD, did not generate dilute-like phenotype in melan-a cells. However, Myo5a-MTD is well colocalized with endogenous Mlph and partially colocalized with melanosome (**Figure 8A**). We reasoned that the presence of both exon-F and exon-G is insufficient for binding to the Mlph occupied by Myo5a, but sufficient for binding to the unoccupied Mlph.

Deletion of exon-F almost eliminated the co-localization of Myo5a-MTD and Mlph (**Figure 8B**), consistent with its essential role for the binding of Myo5a with Mlph. Deletion of exon-G substantially decreased, but did not eliminate, the co-localization of Myo5a-MTD and Mlph (**Figure 8C**), indicating that exon-G plays an auxiliary role for binding of Myo5a with Mlph.

Discussion

It is well-established that Myo5a associates with melanosome via two independent interactions with Mlph, i.e., the interaction between exon-F of Myo5a and Mlph-EFBD and the interaction between the GTD and Mlph-GTBM. In the current study, we identified the third interaction

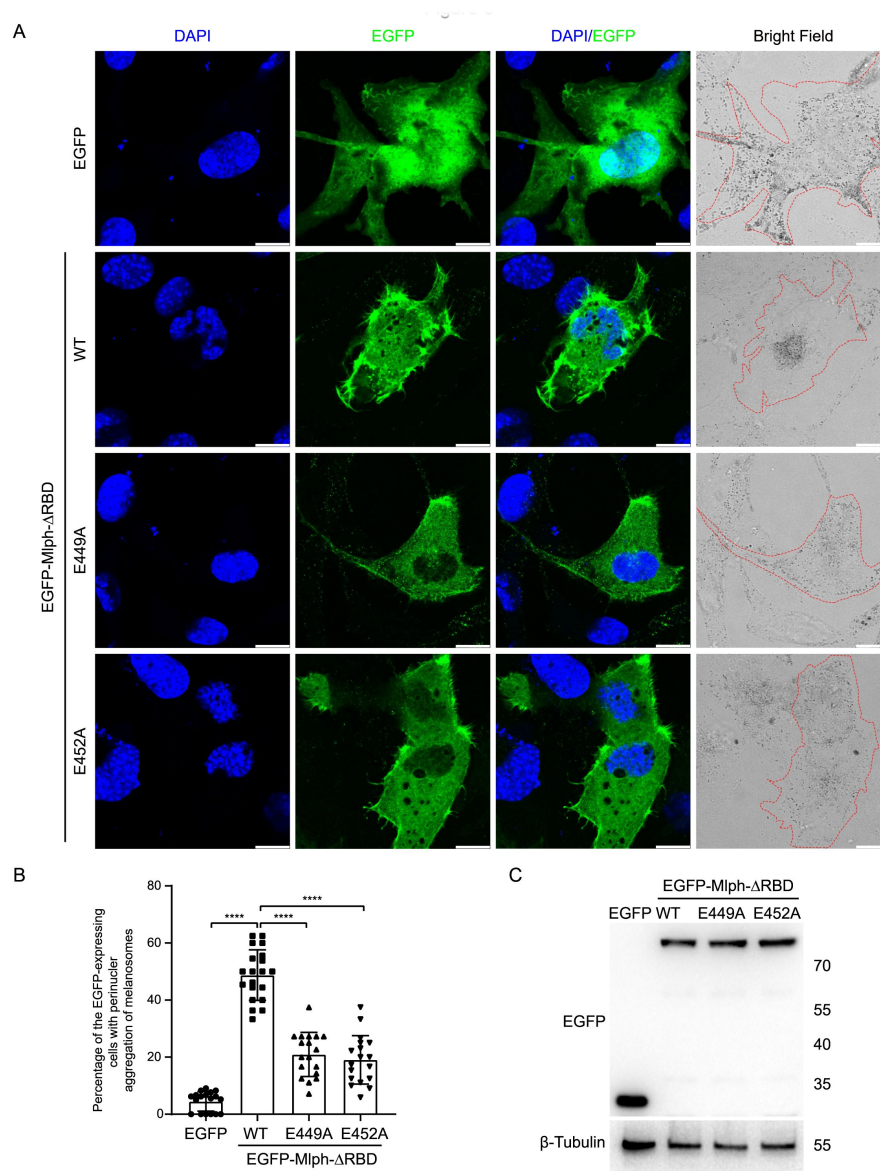


Figure 6.

Both E449 and E452 of Mlph are essential for the perinuclear distribution of melanosomes induced

by **Mlph-ΔRBD overexpression**. Melan-a melanocytes were transfected to express EGFP-Mlph-ΔRBD (WT, E449A, or E452A) or EGFP. The distribution of melanosomes in the transfected melanocytes was imaged and the number of melanocytes with perinuclear distribution of melanosomes was counted. (A) Typical images of melanocytes expressing EGFP alone, EGFP-Mlph-ΔRBD WT, E449A, or E452A. Zooms are x 3. Cells are outlined with red dashed lines. Scale bars = 10 μm. The transfection efficiencies were 11% for EGFP (n=275), 9.2% for EGFP-Mlph-ΔRBD WT (n=194), 11.2% for E449A (n=208), and 11.8% for E452A (n=267). n represents cell number. (B) The percentage of melanocytes exhibiting perinuclear melanosome aggregation among the transfected melanocytes. Results are presented as the mean ± SD of three independent experiments with one-way ANOVA with post-hoc Bonferroni test. Each point represents the percentage of perinuclear distribution of EGFP fusion proteins expressing cells in each fields. ****p<0.0001. (C) Western blot of the lysates of melan-a transfected with EGFP-Mlph-ΔRBD WT, E449A, or E452A. The expressed EGFP fusion proteins were probed with the antibody against EGFP. The relative band densities of EGFP-Mlph-ΔRBD WT, E449A, and E452A were 1, 1.29, and 1.25, respectively. Correction of the transfection efficiencies of those three constructs (Figure 6A, Figure 6-figure supplement) gave rise to the relative protein expression levels of each transfected cells as 1, 1.05, and 0.97 for EGFP-Mlph-ΔRBD WT, E449A, and E452A, respectively.

Figure 6-Source data 1 Original and statistical data for Figure 6 B .

Figure 6-Source data 2 Original and uncropped blots for Figure 6 C .

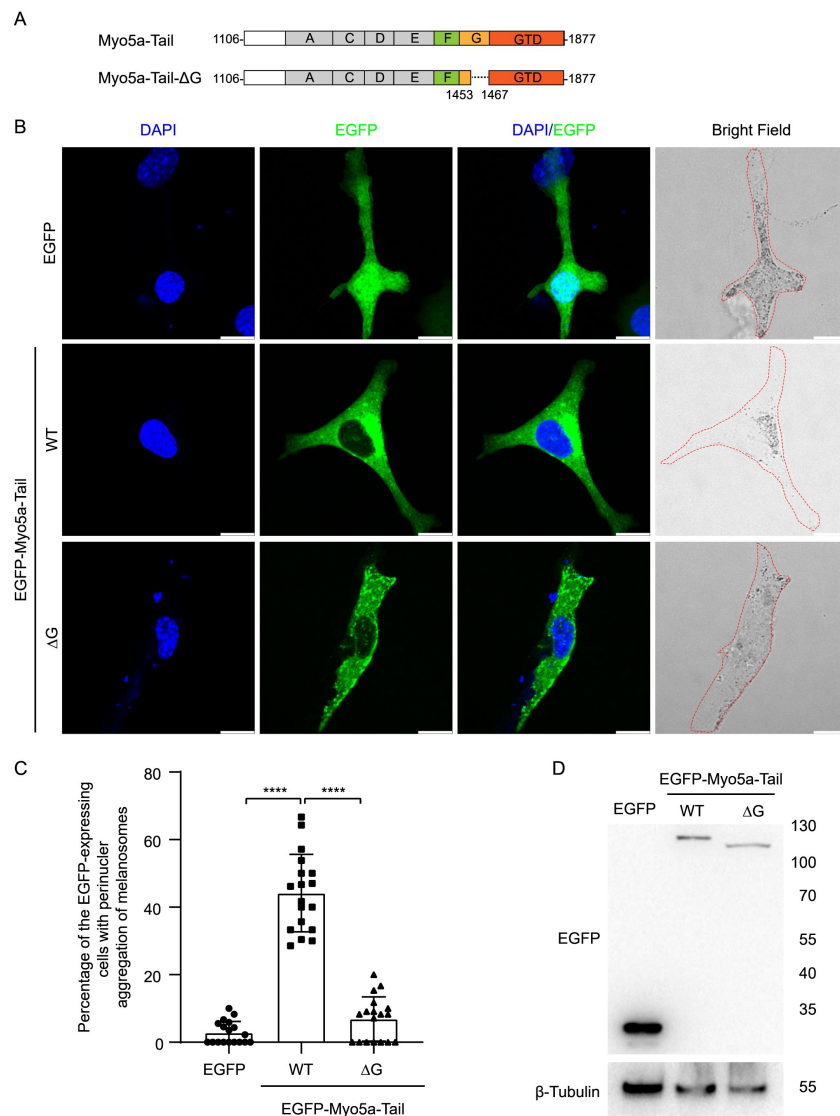


Figure 7.

Exon-G region of Myo5a is essential for the perinuclear distribution of melanosomes induced by Myo5a-Tail overexpression.

(A) Diagram of Myo5a-Tail constructs used for transfecting melan-a melanocytes. (B) Melan-a melanocytes were transfected to express EGFP-Myo5a-Tail and the mutant. The distribution of melanosomes in the transfected melanocytes was imaged and the number of melanocytes with perinuclear distribution of melanosomes was counted. (B) Typical images of melanocytes expressing EGFP-Myo5a-Tail, its mutants, or EGFP. Cells are outlined with a dashed line. Scale bars = 10 μ m. Zooms are $\times 3$. (C) The percentages of melanocytes exhibiting perinuclear melanosome aggregation. Data are the mean \pm SD of three independent experiments with one-way ANOVA with post-hoc Bonferroni test. **** $p < 0.0001$. (D) Western blots of whole cell extracts prepared from melan-a melanocytes transfected with each of the three Myo5a constructs EGFP fusion protein constructs probed with an antibody against EGFP. Each point represents the percentages of perinuclear distribution of EGFP fusion proteins expressing cells in each fields. (D) Western blot of the lysates of melan-a transfected with EGFP-Myo5a-Tail or EGFP-Myo5a-TailΔG. The expressed EGFP fusion proteins were probed with the antibody against EGFP. The relative band densities of EGFP-Myo5a-Tail and EGFP-Myo5a-TailΔG were 1 and 0.9, respectively. Correction of the transfection efficiencies of those three constructs (Figure 7B, Figure 7-figure supplement 1) gave rise to the relative protein expression levels of each transfected cells as 1, 0.93 for EGFP-Myo5a-Tail or EGFP-Myo5a-TailΔG, respectively.

Figure 7-Source data 1 Original and statistical data for Figure 7 C.

Figure 7-Source data 2 Original and uncropped blots for Figure 7 D.

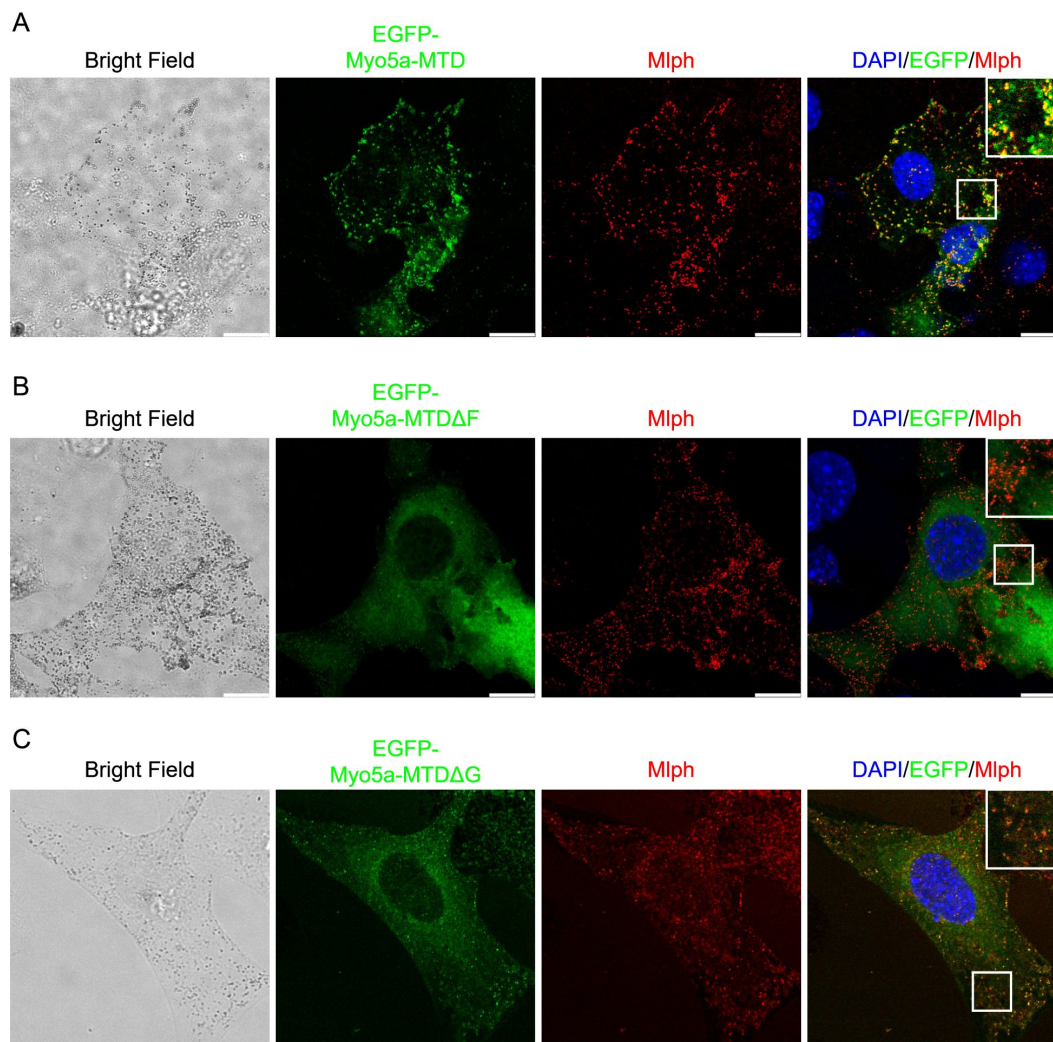


Figure 8.

Effects of deletion of exon-F or exon-G on the localization of Myo5a-MTD in melan-a cells.

Melan-a melanocytes were transfected to express EGFP-Myo5a-MTD (A), EGFP-Myo5a-MTD Δ F (B), or EGFP-Myo5a-MTD Δ G (C) and stained for endogenous Mlph. Insets represent higher magnification photomicrographs of a cell within the region outlined by frames. Scale bars =10 μ m.

between Myo5a and Mlph, i.e., the interaction between the exon-G of Myo5a and the Mlph-ABD. We demonstrated that, similar to the exon-F/EFBD interaction, the exon-G/ABD interaction is also required for the strong binding of Myo5a and Mlph.

Among the three interactions between Myo5a and Mlph, the GTD/GTBM interaction majorly regulates the motor function of Myo5a. At relative high ionic strength but not at physiological ionic strength, Mlph-GTBM binds to the GTD, inducing Myo5a to form the extended conformation and activating Myo5a motor activity (Li et al., 2005 [\[1\]](#); Yao et al., 2015 [\[2\]](#)). At physiological ionic strength, the GTBM-mediated activation of Myo5a depends on the interaction between the GTD and RlpL2, which is regulated by Rab36 (Cao et al., 2019 [\[3\]](#)). Those findings are consistent with the three-dimensional structure of Myo5a-GTD and the folded structure of full-length Myo5a (Niu et al., 2022 [\[4\]](#); Pylypenko et al., 2013 [\[5\]](#); Wei et al., 2013 [\[6\]](#)), in both of which the GTBM-binding sites are buried at the GTD-GTD interface. Upon binding to the RH1 domain of RlpL2, the GTD exposes the GTBM-binding site (Wei et al., 2013 [\[6\]](#)). We therefore proposed that the binding of Rab36/RlpL2 to the GTD exposes the GTBM-binding site, thus facilitating GTBM to bind to the GTD and to activate the motor function of Myo5a (Cao et al., 2019 [\[3\]](#)).

The GTD/GTBM interaction is also required for the stable association between Myo5a and Mlph. The Myo5a tail construct containing all three Mlph-binding sites (the exon-F, the exon-G, and the GTD) produced dominant negative effect in melanocytes, and deleting the GTD abolished the dominant negative effect (**Figure 7** [\[7\]](#) and **8** [\[8\]](#), and reference (X. Wu et al., 2002 [\[9\]](#))).

The exon-F/EFBD and the exon-G/ABD interactions play a major role in the binding of Myo5a with Mlph. Although exon-F and exon-G are adjacent to each other, the exon-F/EFBD interaction and the exon-G/ABD interaction do not interfere with each other. Rather, those two interactions act synergically. We observed that Myo5a-MTD, containing both exon-F and exon-G but lacking the GTD, did not generate a dilute-like phenotype in melanocytes, but was co-localized well with Mlph and partially with melanosomes. Deletion of either exon-F or exon-G substantially weakened the interaction between Myo5a-MTD and Mlph and decreased the colocalization of Myo5a-MTD with Mlph, indicating the both exon-F and exon-G are required for the colocalization.

Our observation that Myo5a-MTD, containing both exon-F and exon-G, was co-localized partially with melanosomes seems to contradict the early work from Hammer laboratory, which showed that MC STK (a Myo5a fragment contains both exon-F and exon-G) did not exhibit any tendency to co-localize with melanosomes (X. Wu et al., 2002 [\[9\]](#)). However, careful examining their image (**Figure 5** [\[10\]](#), in reference (X. Wu et al., 2002 [\[9\]](#))) reveals a partial colocalization of MC STK with melanosomes, particularly at the perinuclear region. It is likely that some melanosome-bound Mlph molecules are unoccupied, some interact with Myo5a via the exon-F/EFBD and the exon-G/ABD interactions but not the GTD/GTBM interaction, and some interact with Myo5a via three interactions. In the former two cases, Myo5a-MTD would be able to bind to the melanosome via Mlph. We therefore conclude that presence of both exon-F and exon-G is sufficient for Myo5a to associate with Mlph, but insufficient for substituting the melanosome-bound Myo5a molecules which bind to Mlph via three distinct interactions.

As discussed above, the GTBM-binding site is buried at the GTD-GTD interface in the folded state of Myo5a, thus is inaccessible for Mlph, and the opening of GTBM-site depends on the interaction with Rab36/RlpL2. On the other hand, the exon-F and the exon-G are likely exposed. We therefore propose that the folded Myo5a first attaches to Mlph via the exon-F/EFBD and exon-G/ABD interactions, then interacts with Rab36/RlpL2 to open the GTBM-site, and finally interacts with the GTBM, forming the extended conformation and being activated.

One interesting finding of this study is that Mlph-ABD was able to separately interact with the exon-G of Myo5a or actin filament, but unable to interact with both of them simultaneously. In other words, Mlph-ABD binds to either exon-G or actin filament. This is consistent with the

geometry of Myo5a, in which exon-G is located far from the motor domain, which interacts with actin filament to produce motility. Given the small size of Mlph-ABD, it is unlikely that Mlph-ABD is able to bridge the exon-G at one end of Myo5a and actin filament which associates with the motor domain located at the other end of Myo5a. An unsolved issue is how Mlph-ABD's interactions with exon-G and actin filament are regulated. *In vitro* studies suggest that the interaction between Mlph-ABD and actin filament might be regulated by phosphorylation (Oberhofer et al., 2017 [DOI](#)).

Based on our current finding and previous studies on the interaction between Myo5a and its associated proteins, we propose following model for the Mlph-mediated Myo5a transportation of melanosome (**Figure 9** [DOI](#)). At stage 1, Mlph associates with melanosome via its interaction with Rab27a, which directly binds to the membrane of melanosome; the unattached Myo5a is in a folded conformation, in which the GTD binds to and inhibits the motor domain. At stage 2, Mlph interacts with the folded Myo5a via the interactions of EFBD/exon-F and ABD/exon-G; the attached Myo5a is still in folded conformation, because the GTBM-binding surface in the GTD is buried at the GTD-GTD interface. At stage 3, the buried

GTBM-binding surface between the GTD-GTD interface is exposed and thus facilitate the binding of GTBM, causing the dissociation of the GTD from the motor domain and inducing the extended conformation of Myo5a (This step is probably regulated by the binding of Rab36/RilpL2 to the GTD). At stage 4, Mlph-ABD dissociates from exon-G and then binds to actin filament, thus enhancing the processive movement of Myo5a (This step might be regulated by the phosphorylation of Mlph-ABD). The interaction between Mlph-ABD and actin filament is regulated by phosphorylation (Oberhofer et al., 2017 [DOI](#)).

Melanosomes in melanocytes are matured through a serial of well-defined morphological steps, from melanin-lacking premelanosomes to blackened melanosomes with melanin fully loaded (Raposo & Marks, 2007 [DOI](#)). During this maturation process, melanosomes undergo microtubule and actin-based transport towards the cell periphery, mediated by different Rab proteins and their effectors (Fukuda, 2021 [DOI](#)). For example, Rab27a mainly associates with intermediate and mature melanosomes (Jordens et al., 2006 [DOI](#)). The melanosome-bound Rab27a in GTP-bound state binds to Mlph, which in turn recruits Myo5a (X. S. Wu et al., 2002 [DOI](#)). We propose that the recruitment of Myo5a by Mlph consists of multiple stages. We expect that Myo5a-MTD, containing both exon-F and exon-G, is able to bind to Mlph at stage 1 and 2, but not at stage 3 and 4, and that Myo5a-Tail, containing all three Mlph-binding sites, is able to bind to Mlph at all four stages.

In conclusion, we demonstrate a direct interaction between the exon-G of Myo5a and the ABD of Mlph, which is essential for the tight binding of Myo5a to Mlph both *in vitro* and *in vivo*. We expect that the melanosomal recruitment and activation of Myo5a are a highly coordinated process mediated by three interactions between Myo5a and Mlph, i.e., the exon-F/EFBD interaction, the exon-G/ABD interaction, and the GTD/GTBM interactions.

Experimental procedures

Materials

Restriction enzymes and modifying enzymes were purchased from New England Biolabs (Beverly, MA), unless indicated otherwise. Actin was prepared from rabbit skeletal muscle acetone powder according to Spudich and Watt (Spudich & Watt, 1971 [DOI](#)). Ni-NTA agarose was purchased from Qiagen (Hilden, Germany). Anti-Flag M2 affinity agarose and HPR conjugated anti-Flag M2 antibody were from Sigma Co. (St. Louis, MO). EGFP and β -Tubulin antibody was purchased from PTMBio (Hangzhou, China). Glutathione(GSH)-Sepharose 4 Fast Flow was from GE Healthcare. FLAG peptide (DYKDDDDK) was synthesized by Augct Co. (Beijing, China). Oligonucleotides were synthesized by Invitrogen Co. (Beijing, China).

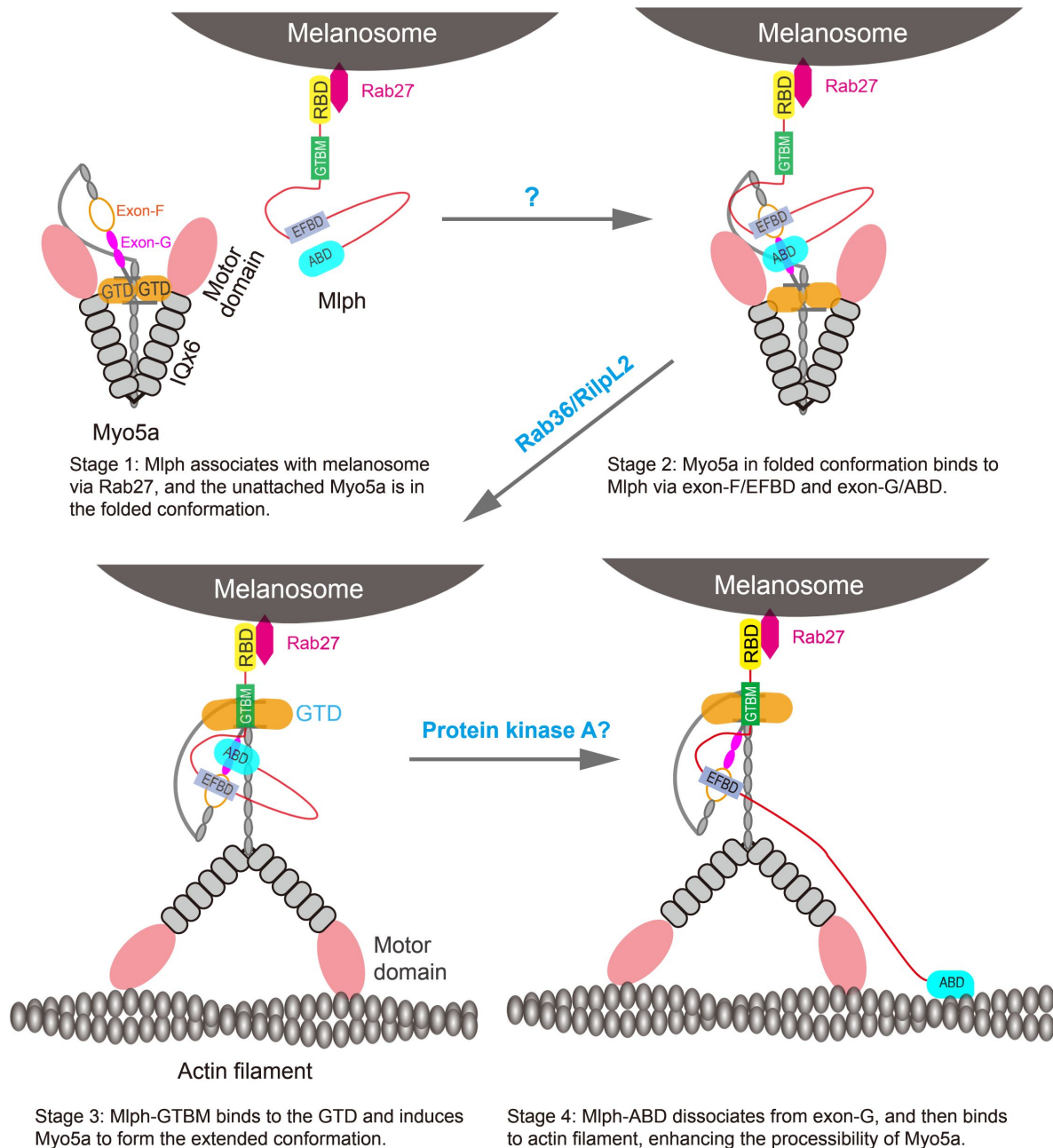


Figure 9.

A model for the Mlph-mediated Myo5a transportation of melanosome.

The Mlph-mediated Myo5a transportation of melanosome is comprised of four stages. At stage 1, Mlph associates with melanosome via its interaction with Rab27a, which directly binds to the membrane of melanosome; the unattached Myo5a is in a folded conformation, in which the GTD binds to and inhibits the motor domain. At stage 2, Mlph interacts with the folded Myo5a via the interactions of EFBD/exon-F and ABD/exon-G; the attached Myo5a is still in folded conformation, because the GTBM-binding surface in the GTD is buried at the GTD-GTD interface. At stage 3, the buried GTBM-binding surface between the GTD-GTD interface is exposed and thus facilitate the binding of GTBM, causing the dissociation of the GTD from the motor domain and inducing the extended conformation of Myo5a (This step is probably regulated by the binding of Rab36/RilpL2 to the GTD). At stage 4, Mlph-ABD dissociates from exon-G and then binds to actin filament, thus enhancing the processive movement of Myo5a (This step might be regulated by the phosphorylation of Mlph-ABD).

Proteins

All Myo5a constructs in this study were created from a melanocyte type Myo5a (Li et al., 2005 [\[4\]](#)). The recombinant proteins of truncated Myo5a containing an N-terminal His-tag and Flag-tag were expressed in BL21(DE3) *E. coli*. The cDNA of truncated Myo5a were amplified by using high-fidelity FastPfu DNA polymerase (TransGen) with Myo5a cDNA as template (Li et al., 2005 [\[4\]](#)), and subcloned into pET30HFa (a modified pET30a vector encoding His-tag and Flag-tag). To improve the expression of short peptides of truncated Myo5a, including Myo5a(1411-1467) and Myo5a(1436-1467), the cDNA of Trx-1 (Genbank ID: P0AA25) was inserted between the Flag-tag sequence and the cDNA of truncated Myo5a in pET30HFa. Myo5a-MTD Δ F were created by using overlap extension PCR with Myo5a-MTD/pFast FTb as template and inserted into pET30HFa. The recombinant proteins were expressed in BL21(DE3) *E. coli* as His-Flag tagged proteins were purified by Ni-agarose affinity chromatography using standard procedures. We also produced an N-terminal His-tagged and Flag-tagged Myo5a-MTD using baculovirus/Sf9 system. The cDNA of Myo5a-MTD was subcloned into the baculovirus transfer vector pFastHFTb (a modified pFastHTb vector containing the His-tag and Flag-tag sequence). Recombinant baculovirus was generated using Bac-to-Bac system. The Myo5a-MTD expressed in Sf9 insect cells was purified by Anti-FLAG M2 affinity chromatography (Li et al., 2008 [\[4\]](#)).

Three truncated Mlph constructs containing an N-terminal GST-tag, including Mlph-ABD (residues 401-590), Mlph- Δ RBD (residues 148-590), Ml-ph- Δ RBD Δ ABD (residues 148-400), were created by subcloning the cDNAs of truncated Mlph into pGEX4Tl vector using BamFII and XhoI sites. Ml-ph-EFBD (residues 241-400) having an N-terminal His-tag and Flag-tag was created by the cDNA of Ml-ph-EFBD subcloning into pET30HFa vector using EcoRI and HindIII sites. Point mutations were created using Fast Mutagenesis System (TransGen) according to the manufacturer's instructions. The recombinant proteins were expressed in BL21(DE3) *E. coli* as His-Flag tagged proteins (in pET30HFa vector) or GST tagged proteins (in pGEX4Tl vector), and purified by Ni-agarose affinity chromatography or GSH-Sepharose affinity chromatography using standard procedures.

Protein pulldown assay

GST pulldown assays were performed as described previously (Zhang et al., 2016 [\[4\]](#)). For GST pulldown of Myo5a-MTD with GST-Mlph-ABD, GSH-Sepharose beads (10 μ l) were mixed with 95 μ l of 2 μ M GST-Mlph-ABD, 4 μ M Myo5a-MTD truncations in Pulldown Buffer-I (5 mM Tris-HCl (pH 7.5), 100 mM NaCl, 1 mM DTT, and 1 mM EGTA, 0.1% NP-40) with rotation at 4 $^{\circ}$ C for 2 h. The GSH-Sepharose beads were then washed three times with 200 μ l of Wash Buffer-I (10 mM Tris-HCl (pH 7.5), 100 mM NaCl, 1 mM DTT, and 1 mM EGTA, 0.1% NP-40), before eluted by Elution Buffer (10 mM GSH, 50 mM Tris-HCl (pH 8.0), 1 mM DTT, and 200 mM NaCl). For GST pulldown of Myo5a-MTD with GST-Mlph- Δ RBD, GSH-Sepharose beads (10 μ l) were mixed with 95 μ l of 2 μ M GST-Mlph- Δ RBD, 4 μ M Myo5a-MTD in Pulldown Buffer-II (5 mM Tris-HCl (pH 7.5), 100 mM NaCl, 1 mM DTT, and 1 mM EGTA) with rotation at 4 $^{\circ}$ C for 2 h. The GSH-Sepharose beads were washed three times with 200 μ l of Wash Buffer-II (10 mM Tris-HCl (pH 7.5), 100 mM NaCl, 1 mM DTT, and 1 mM EGTA) and then eluted by Elution Buffer.

For Flag pulldown assay, Flag-Myo5a-MTD (0.5 μ M) was incubated with 1 μ M GST-tagged Mlph truncations in Pulldown Buffer I and rotated at 4 $^{\circ}$ C for 2 h, mixed with 10 μ l of anti-FLAG M2 agarose. The anti-FLAG M2 agarose were washed three times with 200 μ l of Wash Buffer I. The bound proteins were eluted twice with 20 μ l of 0.1 mg/ml FLAG peptide in Wash Buffer I.

The inputs and the eluted proteins were analyzed by SDS-PAGE and visualized by Coomassie Brilliant Blue (CBB) staining or Western blotting using the indicated antibody. The amounts of pulldowned proteins were quantified using ImageJ (version 1.42Q), and their molar ratios were calculated on the basis of their molecular masses.

Microscale Thermophoresis

The microscale thermophoresis (MST) assay of the interaction between Mlph-ABD with Myo5a-MTD or Myo5a-MTDAG were carried out in a Monolith NT.115 instrument (NanoTemper Technologies, Germany) at 25°C. Mlph-ABD was labelled with ATTO 488 NHS Ester dye (ATTO-TEC) according to the manufacturer's instructions. The Mlph-ABD was kept at a constant concentration of 20 nM. Two-fold dilution series (16 in total) of the Myo5a-MTD (50 µM) or Myo5a-MTDAG (50 µM) were performed in the MST buffer (50 mM Tris-HCl pH 7.8, 100 mM NaCl, 10 mM MgCl₂, 0.05% Tween 20). The dissociation constant K_d was obtained using Monolith Affinity Analysis v2.2.4 software.

Actin cosedimentation assay

Rabbit skeletal actin (2 µM) and Mlph-ABD (4 µM) was incubated in a 60 µL solution of 20 mM Tris-HCl (pH 7.5), 100 mM NaCl, 1 mM EGTA, and 1 mM DTT at 4 °C for 20 min with or without Myo5a-MTD (2 µM). In addition, Myo5a-MTD (0-8 µM) was incubated with rabbit skeletal actin (2 µM) and Mlph-ABD (1 µM) in a 60 µL solution of 20 mM Tris-HCl (pH 7.5), 100 mM NaCl, 1 mM EGTA, and 1 mM DTT at 4 °C for 20 min. The mixtures were centrifuged at 85,000 rpm (Beckman Optima MAX-XP, TLA-120.1 rotor) for 15 min at 4 °C. Equal portions of the pellet and the supernatant were subjected to SDS-PAGE and Coomassie brilliant blue staining.

Melanophilin antibody

To generate a polyclonal antibody against melanophilin, the sequence encoding residues 147-428 of melanophilin (Mlph-147-428) was amplified by PCR using a full-length mouse melanophilin cDNA as template. The PCR product was cloned into pET30a vector and pGEX4T2 vector and expressed in *E. coli* as His-tagged protein (His-Mlph-147-428) and GST-tagged protein (GST-Mlph-147-428), respectively. His-Mlph-147-428 was purified using Ni-NTA agarose chromatography and used for immunizing rabbit. GST-Mlph-147-428 was purified using GSH-Sepharose chromatography. Mlph antibody was affinity-purified from immune sera over a column of GST-Mlph-147-428 coupled to cyanogen bromide-activated Sepharose 4B (GE Healthcare) by standard procedure.

Plasmid constructions for melanocyte transfection

Myo5a-Tail/pEGFP-C1 was produced as described previously (X. Wu et al., 2002 [\[1\]](#)). Myo5a-TailΔF/pEGFP-C1 and Myo5a-TailΔG/pEGFP-C1 were created by overlapping PCR using Myo5a-Tail/pEGFP-C1 as template. Myo5a-MTD/pEGFP-C1 and Myo5a-MTDAG/pEGFP-C1 were produced by PCR amplification using Myo5a-Tail/pEGFP-C1 as template. Myo5a-MTDΔF/pEGFP-C1 was created by subcloning from Myo5a-MTDΔF/pET30a into pEGFP-C1.

Melanocyte culture and transfection

The immortal mouse melanocyte cell line melan-a, kindly provided by Dr. Dorothy Bennett, was cultured as described (Bennett et al., 1987 [\[2\]](#)). Briefly, melan-a cells were cultured in RPMI1640 medium (HyClone) supplemented with 10% fetal bovine serum, 200 nM phorbol 12-myristate 13-acetate and penicillin/streptomycin (1% v/v) in humidified chamber (37 °C, 5% CO₂ incubator). Melan-a cells were passaged at 3-4 day intervals. Hieff Trans® Universal Transfection Reagent (Yeasen) was used for transfection of pEGFP-C1 plasmids into melan-a cells according to the manufacturer's instructions.

Immunocytochemistry

For immunofluorescence staining, melan-a cells were plated on the coverslips. After 24 h culturing, cells were transfected of pEGFP-C1 plasmids. Two days after transfection, the cells were fixed using 4% paraformaldehyde for 20 min, then permeabilized with 0.4% Triton-X in PBS for 15

min. Subsequently, the coverslips were blocked with 1% BSA for 1 h. Melan-a cells were incubated with rabbit antibody against Mlph overnight. Coverslips were washed with PBS for 3 times and then incubated for 1 h at room temperature with secondary antibodies (anti-rabbit IgG coupled with DyLight 549, Jackson). Nuclei were counter-stained with DAPI. coverslips were fixed on glass slides with Fluoromount-GTM (Yeasten). The images were captured by Leica STELLARIS 5 fluorescence microscope.

Footnotes

The abbreviations used are:

- ABD: actin-binding domain of melanophilin
- CaM: calmodulin
- EFBD: exon-F-binding domain of melanophilin
- GSH: glutathione
- GST: glutathione S-transferase
- GTBM: GTD-binding motif of melanophilin
- GTD: globular tail domain of myosin-5a
- Mlph: melanophilin
- MTD: middle tail domain of myosin-5a
- Myo5a: myosin-5a.

Acknowledgements

We thank Dr. Zheng Zhou (Institute of Biophysics, Chinese Academy of Sciences) for advice on myosin-5a/melanophilin interaction. This work was supported by the National Natural Science Foundation of China (31970657).

Conflict of interest

The authors declare that they have no conflicts of interest with the contents of this article.

Author contributions

XdL conceived the study. JP performed most experiments with help from RZ, LLY, NZ and JZ performed the initial experiments demonstrating the interaction between Mlph-ABD and Myo5a tail. QJC prepared melanophilin antibody. SP participated in preparation of recombinant proteins and pulldown assays. JP and XdL designed the study, analyzed the data and wrote the manuscript.

Figure legends

Figure 1-Source data 1 Original and uncropped gels and blots.

Figure 1-Source data 2 Original and uncropped gels and blots.

Figure 2-Source data 1 Original and uncropped gels and blots.

Figure 2-Source data 2 Original and uncropped gels and blots.

Figure 3-Source data 1 Original data.

Figure 3-Source data 2 Original and uncropped gels and blots.

Figure 3-Source data 3 Original and uncropped gels and blots.

Figure 3-Source data 4 Original and uncropped gels and blots.

Figure 4-Source data 1 Original and uncropped gels and blots.

Figure 4-Source data 2 Original and uncropped gels and blots.

Figure 4-Source data 3 Original and uncropped gels.

Figure 5-Source data 1 Original and uncropped gels.

Figure 5-Source data 2 Original and uncropped gels and data.

Figure 6-Source data 1 Original and statistical data.

Figure 6-Source data 2 Original and uncropped blots.

Figure 7-Source data 1 Original and statistical data.

Figure 7-Source data 2 Original and uncropped blots.

Figure 2-figure supplement Source data 1 Original and uncropped gels and blots.

Figure 2-figure supplement Source data 2 Original and uncropped gels and blots.

Figure 2-figure supplement Source data 3 Original and uncropped gels and blots.

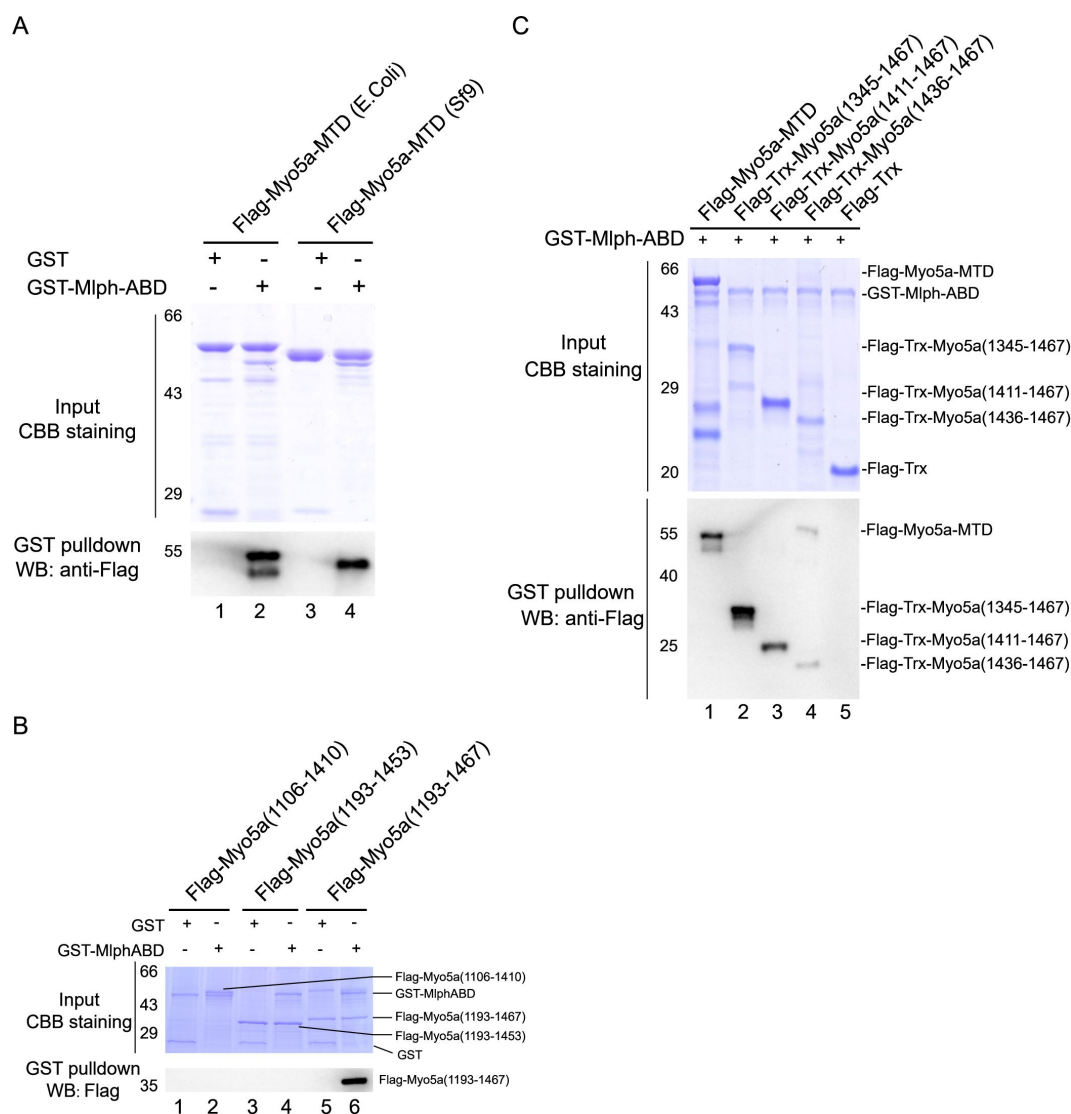


Figure 2-figure supplement

Identification of the Mlph-ABD-bmdmg site in the middle tail of Myo5a.

GST pull-down assays were performed using GST-Mlph-ABD and FLAG-Myo5a-MTD variants. The GSH-Sepharose-bound proteins were eluted by GSH and analyzed by Western blot using anti-FLAG antibody; the inputs were analyzed with SDS-PAGE and visualized by Coomassie brilliant blue (CBB) staining. (A) GST pull-down assays of GST-Mlph-ABD with Flag-Myo5a-MTD expressed in E. coli or Sf9 cells. (B and C) GST pull-down assay of GST-Mlph-ABD with Flag-tagged, truncated Myo5a tail.

Figure 2-figure supplement Source data 1 Original and uncropped gels and blots for Figure 2-figure supplement A.

Figure 2-figure supplement Source data 2 Original and uncropped gels and blots for Figure 2-figure supplement B.

Figure 2-figure supplement Source data 3 Original and uncropped gels and blots for Figure 2-figure supplement C.

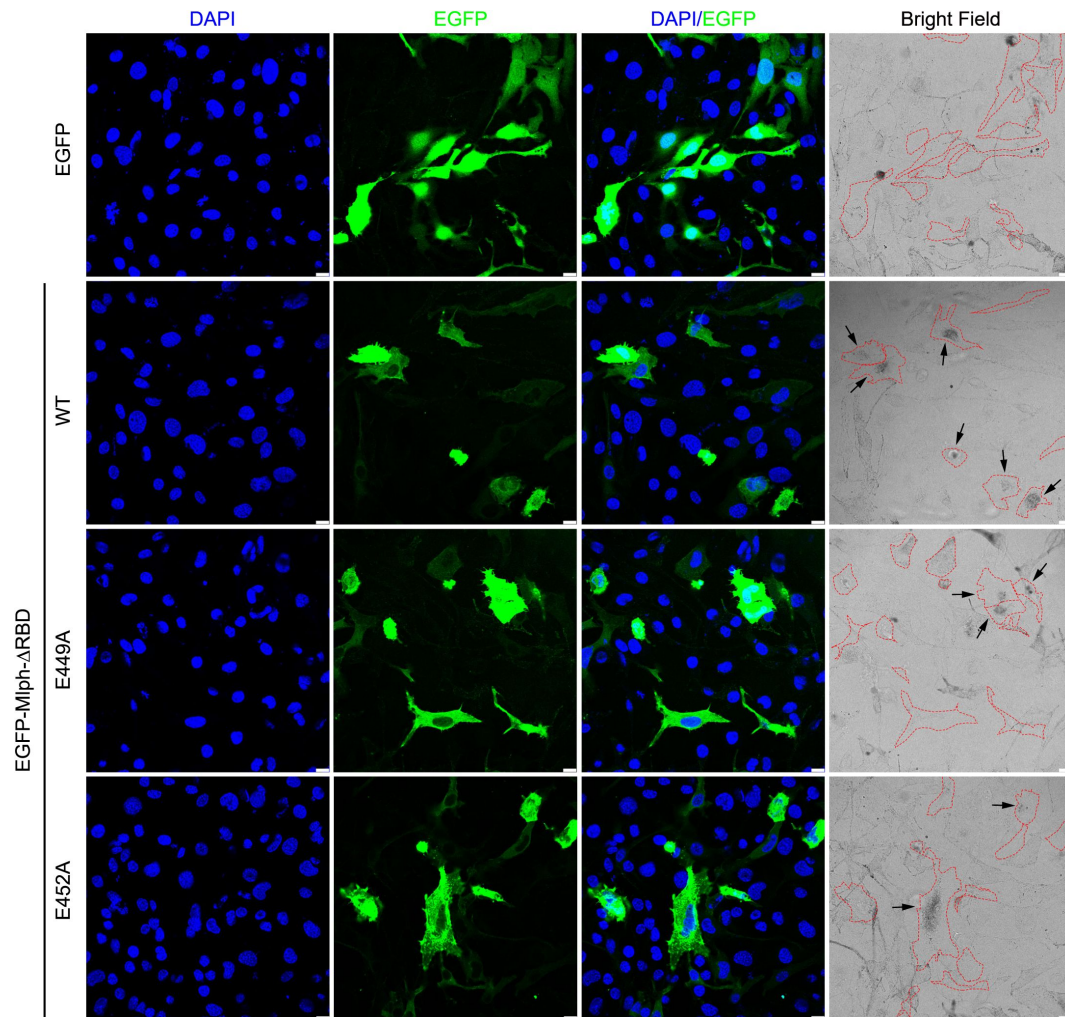


Figure 6-figure supplement

Typical images of melanocytes expressing EGFP-Mlph- Δ RBD, its mutants, or EGFP. Cells are outlined with a red dashed line. Scale bars = 10 μ m. Zooms are $\times 0.75$.

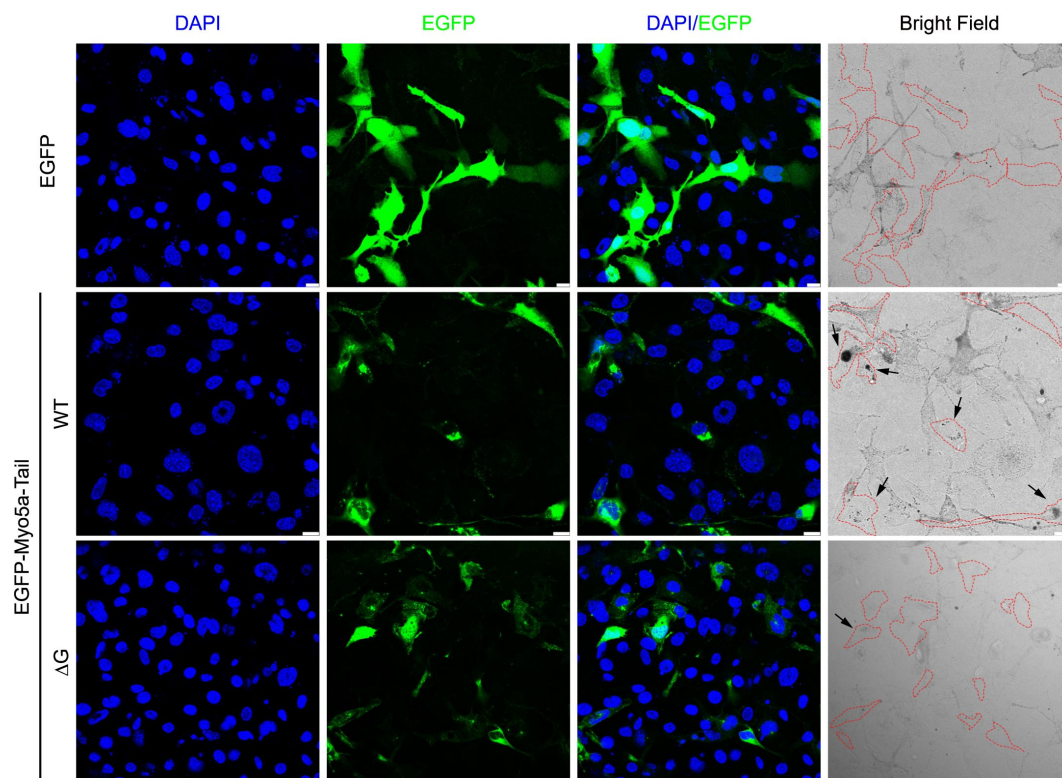


Figure 7-figure supplement

Typical images of melanocytes expressing EGFP-Myo5a-Tail, its mutants, or EGFP. Cells are outlined with a red dashed line. Scale bars = 10 μ m. Zooms are x0.75.

References

- Bennett D.C., Copper P.J., Hart I.R (1987) **A line of non-tumorigenic mouse melanocytes, syngeneic with the B16 melanoma and requiring a tumour promoter for growth** *In J cancer* **39**:414–418
- Cao Q. J., Zhang N., Zhou R., Yao L. L., Li X. D (2019) **The cargo adaptor proteins RILPL2 and melanophilin co-regulate myosin-5a motor activity** *J Biol Chem* **294**:11333–11341 <https://doi.org/10.1074/ibc.RA119.007384>
- Fukuda M (2021) **Rab GTPases: Key players in melanosome biogenesis, transport, and transfer** *Pigment Cell Melanoma Res* **34**:222–235 <https://doi.org/10.1111/pcmr.12931>
- Fukuda M., Itoh T (2004) **Slac2-a/melanophilin contains multiple PEST-like sequences that are highly sensitive to proteolysis** *J Biol Chem* **279**:22314–22321 <https://doi.org/10.1074/ibc.401791200>
- Fukuda M., Kuroda T. S (2002) **Slac2-c (synaptotagmin-like protein homologue lacking C2 domains-c), a novel linker protein that interacts with Rab27, myosin Va/Vñia, and actin** *J Biol Chem* **277**:43096–43103 <https://doi.org/10.1074/ibc.M20386220Q>
- Fukuda M., Kuroda T. S., Mikoshiba K (2002) **Slac2-a/melanophilin, the missing link between Rab27 and myosin Va: implications of a tripartite protein complex for melanosome transport** *J Biol Chem* **277**:12432–12436 <https://doi.org/10.1074/ibc.C200005200>
- Geething N. C., Spudich J. A (2007) **Identification of a minimal myosin Va binding site within an intrinsically unstructured domain of melanophilin** *J Biol Chem* **282**:21518–21528 <https://doi.org/10.1074/ibc.M701932200>
- Huang J. D., Mermall V., Strobel M. C., Russell L. B., Mooseker M. S., Copeland N. G., Jenkins N. A (1998) **Molecular genetic dissection of mouse unconventional myosin-VA: tail region mutations** *Genetics* **148**:1963–1972 <https://doi.org/10.1093/genetics/148.4.1963>
- Hume A. N., Tarafder A.K., Ramalho J.S., Sviderskaya E.V., Seabra M.C. (2006) **A Coiled-Coil Domain of Melanophilin Is Essential for Myosin Va Recruitment and Melanosome Transport in Melanocytes** *Molecular Biology of the Cell* **17**:4720–4735 <https://doi.org/10.1091/mbc.E06-05-0457>
- Hume A. N., Collinson L. M., Rapak A., Gomes A. Q., Hopkins C. R., Seabra M. C (2001) **Rab27a regulates the peripheral distribution of melanosomes in melanocytes** *J Cell Biol* **152**:795–808
- Hume A. N., Seabra M. C (2011) **Melanosomes on the move: a model to understand organelle dynamics** *Biochem Soc Trans* **39**:1191–1196 <https://doi.org/10.1042/BST0391191>
- Ikebe M (2008) **Regulation of the function of mammalian myosin and its conformational change** *Biochem Biophys Res Commun* **369**:157–164 <https://doi.org/10.1016/j.bbrc.2008.01.057>

- Ishida M., Arai S. P., Ohbayashi N., Fukuda M (2014) **The GTPase-deficient Rab27A(Q78L) mutant inhibits melanosome transport in melanocytes through trapping of Rab27A effector protein Slac2-a/melanophilin in their cytosol: development of a novel melanosome-targeting tag** *J Biol Chem* **289**:11059–11067 <https://doi.org/10.1074/jbc.M114.552281>
- Jordens I., Westbroek W., Marsman M., Rocha N., Mommaas M., Huizing M., Lambert J., Naeyaert J. M., Neefjes J (2006) **Rab7 and Rab27a control two motor protein activities involved in melanosomal transport** *Pigment Cell Res* **19**:412–423 <https://doi.org/10.1111/j.1600-0749.2006.00329.x>
- Krementsov D. N., Kremntsova E. B., Trybus K. M (2004) **Myosin V: regulation by calcium, calmodulin, and the tail domain** *J Cell Biol* **164**:877–886
- Kuroda T. S., Ariga H., Fukuda M (2003) **The actin-binding domain of Slac2-a/melanophilin is required for melanosome distribution in melanocytes** *Mol Cell Biol* **23**:5245–5255
- Kuroda T. S., Ariga H., Fukuda M (2003) **The Actin-Binding Domain of Slac2-a/Melanophilin Is Required for Melanosome Distribution in Melanocytes** *Molecular and Cellular Biology* **23**:5245–5255 <https://doi.org/10.1128/mcb.23.15.5245-5255.20Q3>
- Li X. D., Ikebe R., Ikebe M (2005) **Activation of myosin Va function by melanophilin, a specific docking partner of myosin Va** *J Biol Chem* **280**:17815–17822 <https://doi.org/10.1074/jbc.M413295200>
- Li X. D., Jung H. S., Mabuchi K., Craig R., Ikebe M. (2006) **The globular tail domain of myosin Va functions as an inhibitor of the myosin Va motor** *J Biol Chem* **281**:21789–21798 <https://doi.org/10.1074/jbc.M602957200>
- Li X. D., Jung H. S., Wang Q., Ikebe R., Craig R., Ikebe M. (2008) **The globular tail domain puts on the brake to stop the ATPase cycle of myosin Va** *Proc Natl Acad Sci USA* **105**:1140–1145 <https://doi.org/10.1073/pnas.0709741105>
- Li X. D., Mabuchi K., Ikebe R., Ikebe M. (2004) **Ca²⁺-induced activation of ATPase activity of myosin Va is accompanied with a large conformational change** *Biochem Biophys Res Commun* **315**:538–545
- Lindsay A. J., McCaffrey M. W (2014) **Myosin Va is required for the transport of fragile X mental retardation protein (FMRP) granules** *Biol Cell* **106**:57–71 <https://doi.org/10.1111/boc.201200076>
- Liu J., Taylor D. W., Kremntsova E. B., Trybus K. M., Taylor K. A (2006) **Three-dimensional structure of the myosin V inhibited state by cryoelectron tomography** *Nature* **442**:208–211 <https://doi.org/10.1038/nature04719>
- Mehta A. D., Rock R. S., Rief M., Spudich J. A., Mooseker M. S., Cheney R. E (1999) **Myosin-V is a processive actin-based motor** *Nature* **400**:590–593 <https://doi.org/10.1038/23072>
- Nagashima K., Torii S., Yi Z., Igarashi M., Okamoto K., Takeuchi T., Izumi T. (2002) **Melanophilin directly links Rab27a and myosin Va through its distinct coiled-coil regions** *FEBS Lett* **517**:233–238

- Niu F., Liu Y., Sun K., Xu S., Dong J., Yu C., Yan K., Wei Z (2022) **Autoinhibition and activation mechanisms revealed by the triangular-shaped structure of myosin Va** *Sci Adv* **8** <https://doi.org/10.1126/sciadv.add4187>
- Oberhofer A., Spieler P., Rosenfeld Y., Stepp W. L., Cleetus A., Hume A. N., Mueller-Planitz F., Oken Z (2017) **Myosin Va's adaptor protein melanophilin enforces track selection on the microtubule and actin networks in vitro** *Proc Natl Acad Sci USA* **114**:E4714–E4723 <https://doi.org/10.1073/pnas.1619473114>
- Provance D. W., Wei M., Ipe V., Mercer J. A. (1996) **Cultured melanocytes from dilute mutant mice exhibit dendritic morphology and altered melanosome distribution** *Proceedings of the National Academy of Sciences of the United States of America* **93**:14554–14558
- Pylypenko O., Attanda W., Gauquelin C., Lahmani M., Coulibaly D., Baron B., Hoos S., Titus M. A., England P., Houdusse A. M (2013) **Structural basis of myosin V Rab GTPase-dependent cargo recognition** *Proc Natl Acad Sci USA* **770**:20443–20448 <https://doi.org/10.1073/pnas.1314329110>
- Raposo G., Marks M. S (2007) **Melanosomes—dark organelles enlighten endosomal membrane transport** *Nat Rev Mol Cell Biol* **5**:786–797 <https://doi.org/10.1038/nrm2258>
- Rudolf R., Bittins C. M., Gerdes H. H (2011) **The role of myosin V in exocytosis and synaptic plasticity** *J Neurochem* **116**:177–191 <https://doi.org/10.1111/j.1471-4159.2010.07110.x>
- Skolnick M., Kremontsova E. B., Warshaw D. M., Trybus K. M (2013) **More than just a cargo adapter, melanophilin prolongs and slows processive runs of myosin Va** *J Biol Chem* **255**:29313–29322 <https://doi.org/10.1074/jbc.M113.476929>
- Seperack P. K., Mercer J. A., Strobel M. C., Copeland N. G., Jenkins N. A (1995) **Retroviral sequences located within an intron of the dilute gene alter dilute expression in a tissue-specific manner** *EMBO Journal* **74**:2326–2332
- Spudich J. A., Watt S (1971) **The regulation of rabbit skeletal muscle contraction. I. Biochemical studies of the interaction of the tropomyosin-troponin complex with actin and the proteolytic fragments of myosin** *J Biol Chem* **246**:4866–4871
- Strom M., Hume A. N., Tarafder A. K., Barkagianni E., Seabra M. C (2002) **A family of Rab27-binding proteins. Melanophilin links Rab27a and myosin Va function in melanosome transport** *J Biol Chem* **277**:25423–25430 <https://doi.org/10.1074/jbc.M202574200>
- Thirumurugan K., Sakamoto T., Hammer J. A., Sellers J. R., Knight P. J (2006) **The cargo-binding domain regulates structure and activity of myosin 5** *Nature* **442**:212–215 <https://doi.org/10.1038/nature04865>
- Wandinger-Ness A., Zerial M (2014) **Rab proteins and the compartmentalization of the endosomal system** *Cold Spring Harb Perspect Biol* **6** <https://doi.org/10.1101/cshperspect.a022616>
- Wang F., Thirumurugan K., Stafford W. F., Hammer J. A., Knight P. J., Sellers J. R. (2004) **Regulated conformation of myosin V** *J Biol Chem* **279**:2333–2336 <https://doi.org/10.1074/jbc.C30048820Q>

- Wei Q., Wu X., Hammer J. A (1997) **The predominant defect in dilute melanocytes is in melanosome distribution and not cell shape, supporting a role for myosin V in melanosome transport** *J Muscle Res Cell Motil* **18**:517–527
- Wei Z., Liu X., Yu C., Zhang M (2013) **Structural basis of cargo recognitions for class V myosins** *Proc Natl AcadSci USA* **110**:11314–11319 <https://doi.org/10.1073/pnas.1306768110>
- Wu X., Bowers B., Rao K., Wei Q., Hammer J. A. r. (1998) **Visualization of melanosome dynamics within wild-type and dilute melanocytes suggests a paradigm for myosin V function In vivo** *J Cell Biol* **143**:1899–1918
- Wu X., Hammer J. A (2014) **Melanosome transfer: it is best to give and receive** *Curr Opin Cell Biol* **29**:1–7 <https://doi.org/10.1016/i.ceb.2014.02.003>
- Wu X., Rao K., Bowers M. B., Copeland N. G., Jenkins N. A., Hammer J. A (2001) **Rab27a enables myosin Va-dependent melanosome capture by recruiting the myosin to the organelle** *Journal of Cell Science* **114**:1091–1100
- Wu X., Wang F., Rao K., Sellers J. R., Hammer J. A (2002) **Rab27a is an essential component of melanosome receptor for myosin Va** *Mol Biol Cell* **13**:1735–1749 <https://doi.org/10.1091/mbc.01-12-Q595>
- Wu X. S., Rao K., Zhang H., Wang F., Sellers J. R., Matesic L. E., Copeland N. G., Jenkins N. A., Hammer J. A (2002) **Identification of an organelle receptor for myosin-Va** *Nat Cell Biol* **4**:271–278 <https://doi.org/10.1038/ncb760>
- Wu X. S., Tsan G. L., Hammer J. A (2005) **Melanophilin and myosin Va track the microtubule plus end on EB1** *J Cell Biol* **171**:201–207 <https://doi.org/10.1083/icb.200503028>
- Yao L. L., Cao Q. J., Zhang H. M., Zhang J., Cao Y., Li X. D (2015) **Melanophilin Stimulates Myosin-5a Motor Function by Allosterically Inhibiting the Interaction between the Head and Tail of Myosin-5a** *Sci Rep* **5** <https://doi.org/10.1038/srep1Q874>
- Yoshimura A., Fujii R., Watanabe Y., Okabe S., Fukui K., Takumi T (2006) **Myosin-Va facilitates the accumulation of mRNA/protein complex in dendritic spines** *Curr Biol* **16**:2345–2351 <https://doi.org/10.1016/i.cub.2006.10.024>
- Zhang N., Yao L. L., Li X. D (2018) **Regulation of class V myosin** *Cell Mol Life Sci* **75**:261–273 <https://doi.org/10.1007/s00018-Q17-2599-5>
- Zhang W. B., Yao L. L., Li X. D (2016) **The Globular Tail Domain of Myosin-5a Functions as a Dimer in Regulating the Motor Activity** *J Biol Chem* **291**:13571–13579 <https://doi.org/10.1074/jbc.M116.724328>

Article and author information

Jiabin Pan

Group of Cell Motility and Muscle Contraction, State Key Laboratory of Integrated Management of Pest Insects and Rodents, Institute of Zoology, Chinese Academy of Sciences, Beijing 100101, China, University of Chinese Academy of Sciences, Beijing 100049, China

Rui Zhou

Group of Cell Motility and Muscle Contraction, State Key Laboratory of Integrated Management of Pest Insects and Rodents, Institute of Zoology, Chinese Academy of Sciences, Beijing 100101, China, University of Chinese Academy of Sciences, Beijing 100049, China

Lin-Lin Yao

Group of Cell Motility and Muscle Contraction, State Key Laboratory of Integrated Management of Pest Insects and Rodents, Institute of Zoology, Chinese Academy of Sciences, Beijing 100101, China

Jie Zhang

Group of Cell Motility and Muscle Contraction, State Key Laboratory of Integrated Management of Pest Insects and Rodents, Institute of Zoology, Chinese Academy of Sciences, Beijing 100101, China

Ning Zhang

Group of Cell Motility and Muscle Contraction, State Key Laboratory of Integrated Management of Pest Insects and Rodents, Institute of Zoology, Chinese Academy of Sciences, Beijing 100101, China

Qin-Juan Cao

Group of Cell Motility and Muscle Contraction, State Key Laboratory of Integrated Management of Pest Insects and Rodents, Institute of Zoology, Chinese Academy of Sciences, Beijing 100101, China

Shaopeng Sun

Group of Cell Motility and Muscle Contraction, State Key Laboratory of Integrated Management of Pest Insects and Rodents, Institute of Zoology, Chinese Academy of Sciences, Beijing 100101, China, University of Chinese Academy of Sciences, Beijing 100049, China

Xiang-dong Li

Group of Cell Motility and Muscle Contraction, State Key Laboratory of Integrated Management of Pest Insects and Rodents, Institute of Zoology, Chinese Academy of Sciences, Beijing 100101, China, University of Chinese Academy of Sciences, Beijing 100049, China

For correspondence: lixd@ioz.ac.cn

ORCID iD: [0000-0001-8677-9833](https://orcid.org/0000-0001-8677-9833)

Copyright

© 2024, Pan et al.

This article is distributed under the terms of the [Creative Commons Attribution License](https://creativecommons.org/licenses/by/4.0/), which permits unrestricted use and redistribution provided that the original author and source are credited.

Editors

Reviewing Editor

James Sellers

National Institutes of Health, Bethesda, United States of America

Senior Editor

Benoît Kornmann

University of Oxford, Oxford, United Kingdom

Reviewer #1 (Public Review):

Interactions known to be important for melanosome transport include exon F and the globular tail domain (GTD) of MyoVa with Mlph. Motivated by a discrepancy between in vitro and cell culture results regarding necessary interactions for MyoVa to be recruited to the melanosome, the authors used a series of pull-down and pelleting assays experiments to identify an additional interaction that occurs between exon G of MyoVa and Mlph. This interaction is independent of and synergistic with the interaction of Mlph with exon F. However, the interaction of the actin-binding domain of Mlph can occur either with exon G or with the actin filament, but not both simultaneously. These data lead to a modified recruitment model where both exon F and exon G enhance binding of Mlph to auto-inhibited MyoVa, and then via an unidentified switch (PKA?) the actin-binding domain of Mlph dissociates from MyoVa and interacts with the actin filament to enhance MyoVa processivity.

The only weakness noted is that the authors could have had a more complete story if they pursued whether PKA phosphorylation/dephosphorylation of Mlph is indeed the switch for the actin-binding domain of Mlph to interact with exon G versus the actin filament.

<https://doi.org/10.7554/eLife.93662.2.sa1>

Reviewer #2 (Public Review):

The authors identify a third component in the interaction between myosin Va and melanophilin- an interaction between a 32-residue sequence encoded by exon-g in myosin Va and melanophilin's actin binding domain. This interaction has implications for how melanosome motility may be regulated.

The authors have now included some necessary controls that were requested. In terms of adding new information to increase the significance and impact of the paper, they added a single affinity measurement. Unfortunately, it did not involve Exon G specifically. Moreover, they did not add any new mechanistic or functional data to provide a more conceptual advance. For example, is the Exon G interaction regulated by phosphorylation? Is this what dictates the choice between Mlph's actin binding domain (ABD) binding to actin or to exon-G. How does local actin concentration influence this decision. What changes regarding melanosome dynamics in cells between these two alternatives? Do in vitro reconstitution assays show that binding to Exon-G instead of actin affects the processivity of a Rab27a/Myosin 5a/Mlph transport complex? Finally, while the authors make clear in the abstract and text that they are just identifying a third component that mediates the Melanophilin-dependent association of myosin-5a with melanosomes, the title gives the impression that they identified all three in this manuscript. I really think the title should be changed to something like Identification of a third component that mediates the Melanophilin-dependent association of myosin-5a with melanosomes, as this accurately reflects what is new in this work.

<https://doi.org/10.7554/eLife.93662.2.sa0>

Author response:

The following is the authors' response to the original reviews.

We appreciate your comments and suggestions on our manuscript.

In particular, we have measured the affinity between the middle tail domain of myosin-5a (Myo5a-MTD) and the actin-binding domain of melanophilin (Mlph-ABD) using microscale thermophoresis, and obtained the K_d of ~ 0.56 μM , which is similar to the K_d of the globular tail domain of myosin-5a (Myo5a-GTD) to the GTD-binding motif of melanophilin (Mlph-GTBM). Moreover, we have performed Western blot of the lysate of transfected cells, showing that the proteins of the dominant negative construct and the negative control were expressed at similar level without noticeable degradation.

We appreciate the editors' and reviewers' comment on how melanophilin might be regulated in binding to the exon-G of myosin-5 and to actin filaments. Phosphorylation of melanophilin by protein kinase A is one possible mechanism. We will investigate this issues in our future study.

We also took this opportunity to correct several minor errors in the manuscript. Textual alterations can be viewed in the "tracked change" version of the manuscript. Below is the comments from the editors and the two reviewers together with our point-by-point responses.

eLife assessment

This study represents a useful description of a third interaction site between melanophilin and myosin-5a which is important in regulating the distribution of pigment granules in melanocytes. While much of the data forms a solid case for this interaction, the inclusion of important controls for the cellular studies and measurement of interaction affinities would have been helpful.

Public Reviews:

Reviewer #1 (Public Review):

Interactions known to be important for melanosome transport include exon F and the globular tail domain (GTD) of MyoVa with Mlph. Motivated by a discrepancy between in vitro and cell culture results regarding necessary interactions for MyoVa to be recruited to the melanosome, the authors used a series of pull-down and pelleting assays experiments to identify an additional interaction that occurs between exon G of MyoVa and Mlph. This interaction is independent of and synergistic with the interaction of Mlph with exon F. However, the interaction of the actin-binding domain of Mlph can occur either with exon G or with the actin filament, but not both simultaneously. These data lead to a modified recruitment model where both exon F and exon G enhance the binding of Mlph to auto-inhibited MyoVa, and then via an unidentified switch (PKA?) the actin-binding domain of Mlph dissociates from MyoVa and interacts with the actin filament to enhance MyoVa processivity.

The only weakness noted is that the authors could have had a more complete story if they pursued whether PKA phosphorylation/dephosphorylation of Mlph is indeed the switch for the actin-binding domain of Mlph to interact with exon G versus the actin filament.

We thank Reviewer #1 for careful reading of the manuscript and appreciation of the study. We agree with the Reviewer that it is important to understand how the actin-binding domain of Mlph switch its interaction with the exon-G of Myo5a and actin filament. We would like to pursue this direction in our future research.

Reviewer #2 (Public Review):

The authors identify a third component in the interaction between myosin Va and melanophilin- an interaction between a 32-residue sequence encoded by exon-g in myosin Va and melanophilin's actin-binding domain. This interaction has implications for how melanosome motility may be regulated.

While this work is largely well done and certainly publishable following needed revisions (e.g. some affinity measurements, necessary controls for the dominant negative experiments), I believe that additional work would be required to make a more compelling case. First, the study provides just one more piece to a well-developed story (the role of exon-F and the GTD in myosin Va: melanophilin (Mlph) interaction), much of which was published 20 years ago by several labs. Second, the study does not demonstrate a physiological significance for their findings other than that exon-G plays an auxiliary role in the binding of myosin Va to Mlph. For example, what dictates the choice between Mlph's actin binding domain (ABD) binding to actin or to exon-G. Is it a PTM or local actin concentration? It is unlikely to be alternative splicing as exon-G is present in all spliced isoforms of myosin Va. And what changes re melanosome dynamics in cells between these two alternatives? Similarly, the paper does not provide any in vitro evidence that binding to exon-G instead of actin effects the processivity of a Rab27a/Myosin Va/Mlph transport complex. For example, if the ABD sticks to exon-G instead of actin, does that block Mlph's ability to promote processivity through its interaction with the actin filament during transport? In summary, given that the authors did not directly test their model either in vitro or in cells, I do not think this story represent a significant conceptual advance.

We thank Reviewer #2 for careful reading of the manuscript and the suggestions of improving the manuscript. As suggested by the reviewer, we have measured the affinity between the middle tail domain of Myo5a (Myo5a-MTD) and Mlph-ABD (Kd ~0.562 uM), which is similar to that between the globular tail domain of Myo5a (Myo5a-GTD) and the GTBM of Mlph. In addition, we have performed additional experiments showing the integrity and the expression level of the dominant negative constructs in the transfected cells.

We believe more extensive experiments are required to address other questions raised by the reviewer. For example, what dictates the choice between Mlph's actin binding domain (ABD) binding to actin or to exon-G is an open question. As we proposed, phosphorylation by protein kinase A is only one possible mechanism. We would like to pursue them in our future research.

The reviewing editor feels strongly that addressing some of the points raised by the reviewers would make this a more compelling manuscript. In particular, a measurement of the affinity of the relevant fragments from melanophilin and myosin-5a would indicate that the interaction might be physiologically relevant. Concerning the dominant negative experiments, the lack of effect of an expressed fragment could be that the expressed fragments were simply degraded or expressed at too low of a level to be competing. The reviewer gives guidelines on how to address this. Reviewer #2 made a point that it would be compelling if the effect of phosphorylation as suggested in the model was tested, but we all agree that this could well be the subject of a later study. In addition, the authors make a very interesting proposal for how protein kinase A could be involved in this regulation as has been suggested previously. Perhaps the use of phosphomimetic mutations could give some insight into this. Such experiments, if consistent with the proposed model would certainly raise the impact of this study. Finally, a very clear periodicity in hydrophobic amino acids is apparent

Recommendations for the authors:

The reviewing editor feels strongly that addressing some of the points raised by the reviewers would make this a more compelling manuscript. In particular, a measurement of the affinity of the relevant fragments from melanophilin and myosin-5a would indicate that the interaction might be physiologically relevant. Concerning the dominant negative experiments, the lack of effect of an expressed fragment could be that the expressed fragments were simply degraded or expressed at too low of a level to be competing. The reviewer gives guidelines on how to address this. Reviewer #2 made a point that it would be compelling if the effect of phosphorylation as suggested in the model was tested, but we all agree that this could well be the subject of a later study. In addition, the authors make a very interesting proposal for how protein kinase A could be involved in this regulation as has been suggested previously. Perhaps the use of phosphomimetic mutations could give some insight into this. Such experiments, if consistent with the proposed model would certainly raise the impact of this study. Finally, a very clear periodicity in hydrophobic amino acids is apparent in the interacting sequences of both Myo5

(yrisLykrMidLmeqLekqdkVrkLkkqLkvFakkIgeLevgqmen) and Mlph (tdeeLseMedrVamtAseVqqAeseIsdIesrIaaLra). This is strongly suggesting a leucine-zipper-like coiled coil, rather than an interaction mediated solely by charge. Recent softwares (and easily accessible too) like AlphaFold multimer might yield important structural insight into the binding configuration and might help rationalize the effect of the mutations herein.

We thank the editors and the reviewers for their suggestions of improving the manuscript. We have performed the several essential experiments to address the concerns raised by the reviewers.

(1) Regarding the affinity of the relevant fragments from melanophilin and myosin-5a. We have measured the affinity between Mlph-ABD and Myo5a-MTD using MST (Kd ~562 nM) (see revised Figure 3A).

(2) Regarding the concerns on the dominant negative experiments. We have examined the molecular sizes and expression levels of Mlph or Myo5a constructs by Western blots. First, we show that all constructs have correct molecular size in transfected cells (see revised Figure 6C and 7D), indicating that the inability of Myo5a or Mlph truncations to generate dilute-like phenotypes was not due to the intracellular degradation of the EGFP fusion protein. Second, by correcting for the percentage of transfected cells, we show that the overall expression levels of the wild-type construct and the mutants are roughly equal. Third, we categorized the expression levels into high and low, and calculated percentage of the DN phenotype in high and low expression levels. The results are consistent with the percentage of DN phenotype in total EGFP fusion protein cells.

(3) Regarding the suggestion to investigate the effect of phosphorylation by protein kinase A on Mlph-ABD's interaction with Myo5a and actin filament. We understand that it is important to elucidate the mechanism by which the actin-binding domain of Mlph switch its interaction with the exon-G of Myo5a and actin filament. However, as we proposed, phosphorylation by protein kinase A is one possible mechanism, and more extensive experiments are required to address this question. Therefore, we would like to pursue it in our future research.

(4) Regarding the suggestion to predict the interaction between the exon-G of myosin-5a and Mlph-ABD using AlphaFold. We have used AlphaFold multimer to predict the Myo5a-MTD/Mlph-ABD interaction. Remarkably, the AlphaFold predicted that the binding of Myo5a-MTD with Mlph-ABD is mediated by an antiparallel coiled-coil formed by Myo5a (1430-1467) and Mlph (450-481), just as predicted by the editors. This prediction is also consistent with our finding that the exon-G of Myo5a interacts with Mlph-ABD. However, the predicted model cannot explain our mutagenesis results. We will pursue this point in the future research.

Nevertheless, we are grateful to the editors for bringing this idea to our attention, because it will help us to design experiments to investigate the nature of Myo5a-exon-G/Mlph-ABD interaction.

Reviewer #1 (Recommendations For The Authors):

Specific minor comments

Q1: In figs 6-7 an overlay between DAPI and EGFP would be helpful for the reader to see perinuclear distribution.

As suggested, we have added the merged images of DAPI and EGFP in the revised Figure 6 and 7.

Q2: The delta symbol in the pdf text was corrupted.

The corrupted delta symbol has been fixed in the revised manuscript.

Reviewer #2 (Recommendations For The Authors):

Q1: Please explain in detail early in the text what exon-G is - length, position in the tail, and evidence that it is a coiled coil (CC). Of note, is it only long enough for about 4 heptad repeats? Has it been shown biochemically to form a CC? Is the CC irreversible? What would be the consequence of removing the exon-G CC on the ability of surrounding regions to bind Mlph (exon-F and the GTD)?

We thank the reviewer for this suggestion. In the revision, we added a new paragraph (the first paragraph in the results section) and revised Figure 1A to introduce the middle tail domain and alternatively spliced exons of Myo5a.

Exon-G is 32 amino acids in length, located at the C-terminal region of the middle tail domain, immediately before the globular tail domain. Exon-G region was predicted to form a short coiled-coil by using on-line tools (such as paircoil), and this prediction has not been tested biochemically. Moreover, we do not know whether the exon-G coiled-coil is reversible or not.

We have not examined the effect of removing the whole exon-G on the interaction between the GTD and Mlph-GTBM. The exon-G (residues 1436-1467) and the GTD core (residues 1498-1877) are separated by a long loop of 31 residues. We therefore expect that the removing the exon-G will not affect the GTD/Mlph-GTBM interaction.

Physically, exon-F is immediately followed by exon-G, and those two regions might interfere with each other. In our preliminary study, we found that removing the whole exon-G abolished the interaction between exon-F and Mlph-EFBD. On the other hand, removing the C-terminal half (residues 1454-1467) of exon-G had little effect the interaction between exon-F and Mlph-EFBD (see Figure 2C). In this work, we intentionally selected the later construct for functional analysis of the exon-G/Mlph-ABD interaction, because removing the C-terminal half of exon-G abolishes the interaction with Mlph-ABD, but does not affect the exon-F/Mlph-EFBD interaction.

Q2: Figures 1-3. While the pulldown experiments demonstrating an interaction between Mlph-ABD residues 446-571 and Myo5a-MTD are a good start, one would like to see affinity measurements to gauge the likelihood that this interaction is physiologically relevant. The same goes for the pulldown experiments demonstrating an interaction between (i) the C-terminal half of exon-G (residues 1453-1467) and the Mlph-ABD, (ii) between residues 1411-1467 (a short peptide containing exon-F and exon-G) and the Mlph-ABD, and (iii) between residues 1436-1467 (a short peptide containing exon-G) and

the Mlph-ABD. This would also apply to the pulldowns in 3C-3E where versions of the proteins with charge residue changes were tested.

We agree the reviewer's opinion that determination of the affinities between Mlph-ABD and Myo5a-MTD and their variants will be helpful in understanding the physiological relevance of Exon-G/Mlph-ABD interaction. However, the extensive experiments suggested by the reviewer require many high quality, purified proteins, which are not trivial.

Nevertheless, we think it is important to know the affinity between Myo5a-MTD and Mlph-ABD (both wild-type), as this parameter can be used for the comparison of the three interactions between Myo5a and Mlph. Therefore, we have obtained the affinity between Myo5a-MTD and Mlph-ABD using microscale thermophoresis (MST). The dissociation constant (Kd) of Myo5a-MTD to Mlph-ABD is 0.562 ± 0.169 μ M, which is similar to that between Myo5a-GTD and Mlph-GTBM (~ 1 μ M) (Geething & Spudich (2007) JBC 282:21518). Consistent with GST pulldown results, MST shows that deletion of C-terminal half of exon-G (1453-1467) greatly decreases the MST signals (see revised Figure 3A).

Q3: While the domain negative (DN) approach to testing functional significance is OK, rescuing dilute/myosin Va null melanocytes with full-length myosin Va containing the various deletions would have been more convincing. Also, the authors must show (i) that the DN constructs are the correct size in transfected cells (i.e. are not degraded), and (ii) that they are expressed at roughly equal levels (either by doing Westerns and correcting for the percent of transfected cells, or by measuring total cellular fluorescence in transfected cells). Without this information, it remains possible that constructs not exhibiting a DN effect are simply degraded or poorly expressed. This applies to all the DN data in Figures 6 and 7.

We agree with the reviewer that Myo5a null melanocytes is ideal for investigating exon G function. Unfortunately, we do not have Myo5a null melanocytes derived from dilute mice.

To confirm the integrity of the overexpressed proteins in the transfected cells, we performed Western blot of those proteins, including EGFP-Mlph- Δ RBD (wild-type and two mutants) and Myo5a-Tail (wild-type and Δ G mutant), in the lysate of the transfected cells. Western blots show that all those proteins have correct molecular masses, indicating no degradation of those overexpressed proteins (see revised Figure 6C and 7C). Moreover, by correcting for the percentage of transfected cells, we show that the overall expression levels in each transfected cell of the wild-type construct and the mutants are roughly equal. This information is included in the revised manuscript (Line 222-225; 237-241).

Q4: The authors scored the DN phenotype as yes/no but it mostly likely varies depending on the degree of over-expression. Showing that the degree of melanosome centralization scales with the degree of overexpression, and that the correlation between expression level and phenotype varies depending on the construct would strengthen the results.

We agree with the reviewer's prediction that the degree of DN phenotype should depend on the of over-expression level. We analyzed the EGFP signals of transfected cells and found very few cells with medium expression level. Therefore, we simply categorized the expression levels into high and low, and calculated the DN phenotype in each categories as shown in the table below. These results are consistent with the expectation that the degree of DN phenotype depends on the over-expression level of the transfected constructs.

Author response table 1.

Percentage of the EGFP-expressing cells with perinuclear aggregation of melanosomes

Transfected construct	High expression	Low expression
EGFP-Mlph-ΔRBD WT	59.2% (n = 94)	23.8% (n = 74)
EGFP-Mlph-ΔRBD E449A	22.5% (n = 103)	4.9% (n = 71)
EGFP-Mlph-ΔRBD E452A	20.8% (n = 120)	3.7% (n = 77)
EGFP-Myo5a-Tail	69.3% (n = 96)	11.9% (n = 63)
EGFP-Myo5a-TailΔG	16.7% (n = 110)	2.1% (n = 72)

n, cell numbers.

Q5: The conclusion from the data in Figure 8A- "the presence of both exon-F and exon-G is insufficient for binding to the Mlph occupied by Myo5a, but sufficient for binding to the unoccupied Mlph"- should be verified by also doing the experiment in myosin Va knockdown cells.

We agree. Unfortunately, our RNAi knockdown of Myo5a in melanocytes by RNAi is not ideal and we do not have Myo5a knockout melanocytes. We will pursue this point in the future.

Q6: Line 213 "three Mlph-binding regions, i.e., exon-F, exon-F, and GTD (Figure 7A)" has a typo.

This typo has been corrected.

Q7: The authors should provide high mag insets for the images in Figure 8.

As suggested, we have revised Figure 8 by including high mag insets for the images.

<https://doi.org/10.7554/eLife.93662.2.sa3>